Modulation/Demodulation Techniques for Satellite Communications

Part III: Advanced Techniques — The Nonlinear Channel

Jim K. Omura
Marvin K. Simon

October 1, 1982

NASA

Modulation/Demodulation Techniques for Satellite Communications

Part III: Advanced Techniques — The Nonlinear Channel

Jim K. Omura
Marvin K. Simon

October 1, 1982

ABSTRACT

Part III of this report presents a theory for deducing and predicting
the performance of transmitter/receivers for bandwidth efficient modulations
suitable for use on the nonlinear satellite channel. The underlying principle
used throughout is the development of receiver structures based on the maximum-
likelihood decision rule and approximations to it. Along with this overall
theme is the desire to apply the bit error probability transfer function
bounds developed in great detail in Part IV to these modulation/demodulation
techniques. The effects of the various degrees of receiver mismatch are
considered both theoretically and by numerous illustrative examples.

CONTENTS

Figures

1.0 Introduction

Here in Part III we generalize the results of Part II for the linear channel to apply to nonlinear satellite channels. In particular, we examine the general class of bandwidth efficient modulation techniques and their error probability evaluation for the nonlinear satellite channel model.

First, we define the mathematical model for the nonlinear satellite channel that will be used throughout this part of the report. Next, we briefly review the maximum-likelihood (ML) criterion for the linear channel and show how the previously derived bit error bounds for the ideal ML receiver can be modified so as to apply to a mismatched receiver, i.e., one in which the metric it uses is not ML for the actual channel. These results are then generalized to the case of a nonlinear satellite channel. Finally we examine an approximation approach to designing a ML receiver for this type of channel.

1.1 Historical Background

For many years analysts have grappled with the problem of computing the performance of digital modulations transmitted over a nonlinear channel perturbed by a host of different types of interference. Early in the game, investigators realized that many of the analysis techniques that were suited to computing the performance of these modulations over a linear channel perturbed by the same sources of interference could also be applied to the nonlinear channel provided that the nonlinearity was appropriately modelled, e.g., as a zero memory device. As such it is not surprising to find t   much of the reported research on the subject of performance over nonlinear interference channels draws upon previously reported contributions for performance over the analogous linear channel. This is not to say that the actual computation of performance over the nonlinear channel is a simple and direct extension of the similar results for the linear channel. In fact, the functional form and the mathematics needed to arrive at these forms are typically quite different for the two types of channels.

As an example of the above, we cite first the inclusive work of Shimbo, Fang, and Celebiler [1] and Fang and Shimbo [2]* which investigate the performance of a variety of coherent phase-shift-keyed (CPSK) signals over a linear channel perturbed

*This paper also provides an excellent bibliography of earlier work on the subject.

1

by additive Gaussian noise and both intersymbol and cochannel interferences. The method employed in these papers for evaluating the average probability of error was to characterize the intersymbol interference in terms of its characteristic function and then expand this function into a power series. Using this approach, Ekanayake and Taylor [3] analyzed the performance of CPSK signalling over a non-linear (specifically a hard-limited) channel in the presence of uplink (prior to the nonlinearity) and downlink (following the nonlinearity) additive Gaussian noises (assumed to be independent of one another) and intersymbol interference. The expression for the average error probability is obtained in the form of an infinite series as a function of expected values of trigonometric functions of the interference and uplink noise. These expected values are in turn obtained from the power series expansion of the interference's characteristic function as mentioned above. When the intersymbol interference is set to zero, the infinite series in [3] identically reduces to an earlier result for the same hard-limited channel obtained by Jain and Blachman [4].

As one continues to search through the literature on nonlinear satellite channels, he finds that the majority of the work falls into two categories:* (1) modelling of the nonlinearity, and (2) evaluation of error probability performance of the receiver. The previously mentioned references clearly fall into the second category. Before continuing with other important contributions to this category we shall briefly digress to mention several researchers whose work is appropriate to the first category and without whose efforts the performance evaluations would not be possible.

As previously mentioned the success of many of the error probability performance analysis techniques rests heavily on the ability to represent the non-linearity as a zero memory device. While a hard-limiter clearly falls in this category and is trivial to model, a travelling wave tube (TWT) amplifier typically employed in satellite transponders requires a significantly more complex mathematical model. A TWT amplifier exhibits, in general, two nonlinear distortion effects; a nonlinear input-output power (AM/AM conversion) effect and a nonlinear output phase-input power (AM/PM conversion) effect. An amplitude-phase model for the TWT is one which directly models these conversion characteristic in mathematical form [5-8]. A quadrature model for the TWT produces an output signal

---

*Another important category, although not of interest in this report, is the evaluation of intermodulation distortion for a multiple carrier system.

2

having the above distortions by passing the input signal and a 90° phase shift of it through separate envelope nonlinearities. The outputs of these nonlinearities are then summed to produce the signal with the desired AM/AM and AM/PM characteristics. This model as originally suggested by Kaye, et al., [9] used a power series method to approximate the two envelope nonlinearities [10]. Later, Hetrakul and Taylor [11,12,13] used a Bessel function approximation which had the advantage of requiring a much smaller number of approximating coefficients (4 as compared to 16) to give an accurate fit to the measured TWT characteristics. Most recently, Saleh [14] was able to further reduce the number of parameters needed for either the amplitude-phase or the quadrature model. In particular, simple two-parameter formulas were developed for each of the four aforementioned functions (i.e., AM/AM and AM/PM characteristics, and the two envelope nonlinearities in the quadrature model) which had the further advantage of fitting TWT measurements more accurately than previously reported formulas. The method in [14] also permitted a closed-form solution of the output signal for an input signal consisting of two phase-modulated carriers, and a solution containing a single integral when more than two such carriers are involved. Such solutions are valuable in performing intermodulation distortion analyses in nonlinear satellite systems [15].

Returning now to the work pertaining to error probability performance evaluation, we begin by citing several contributions [4,12,16] dealing with performance of CPSK over wide-band nonlinear channels. The term "wide-band" is used to identify the fact that in all of these cases the transmission bandwidth was assumed sufficient so as to pass the signals of interest with negligible degradation due to intersymbol interference. In an effort to remove this oversimplifying assumption and at the same time allow for the inclusion of both uplink and downlink noises simultaneously, we next cite the pioneering work performed at LinCom Corporation under the direction of Dr. William C. Lindsey first reported in [17], and later in the open literature along with extensions thereof [18-21]. Several different mathematical approaches for evaluating the error probability in the presence of these various interference sources were presented there for each of several receiver implementations. In particular, a memoryless receiver which makes its decision based on a single sample basis after coherent demodulation by quadrature phase-coherent carriers was first considered. Following this, results were presented for a memory-type receiver referred to as a maximum-likelihood

sequence estimator (MLSE) and implemented by the Viterbi algorithm [22]. Discussions of this type of demodulator for linear intersymbol interference channels can be found in several excellent papers by Forney [23], Ungerboeck [24] and Hayes [25]. For the nonlinear intersymbol interference channel, with no uplink noise, Mesiya, et al., [26] has also evaluated the performance of a MLSE receiver for binary CPSK signals. Similarly, Forney, et al., [27] have extended the results in [4] for the memoryless receiver to a two-link channel with M-ary PSK signalling and arbitrary AM/AM and AM/PM channel nonlinearities.

More recently, attention [28-36] has turned to reduced complexity Viterbi demodulators for applications (e.g., voiceband data transmission) where the number of interfering symbols is large. In effect, the receiver assumes that the channel (linear or nonlinear) memory is much less than it really is and as such ignores some of the channel's intersymbol interference. Several approaches have been suggested in the above references for choosing the state variables which characterize the truncated state form of Viterbi detector.

In all our discussions thus far, the emphasis has been on the conventionality of the receiver with less attention paid to its optimality. As such, the receiver was always _mismatched_ to the channel and hence its performance was always degraded relative to that of the optimum receiver. Optimum (maximum-likelihood) receivers for nonlinear satellite channels with various combinations of intersymbol interference, uplink, and downlink noises have been investigated in recent years. In [37], a Volterra series approach was applied to find ML receivers for channels that include a power-law nonlinearity, intersymbol interference, and downlink noise only. The first attempt to derive a ML receiver for a channel including both uplink and downlink noises, but no intersymbol interference was presented in [38]. The most comprehensive work on optimum receivers for nonlinear channels with arbitrary AM/AM and AM/PM conversion characteristics and all three interference sources (intersymbol, uplink, and downlink noises) present simultaneously was recently reported in [39] and [40]. There the form of the optimum (MLSE) receiver was derived and its symbol error probability evaluated. Since the computation of the likelihood ratio, and hence the metric to be used by the detector, were not easily obtained in closed form, two approximate forms of the optimum receiver were derived and analyzed, using a combination of Chernoff and generating function techniques such as those discussed in Part IV of this report. For

4

binary CPSK transmission. It was shown that even moderate-complexity approximations allow a power saving of more than one dB with respect to conventional structures.

Finally, we would like to point out the existence of a recent "mini"-issue of the IEEE Transactions on Communications [4] which contains many fine contributions on the subject of communications over nonlinear channels one of which was already cited as [2].

2.0   Satellite Channel Model

A model for the transponder satellite channel is sketched in Figure 1. This channel model consists of an uplink additive white Gaussian noise plus interference,
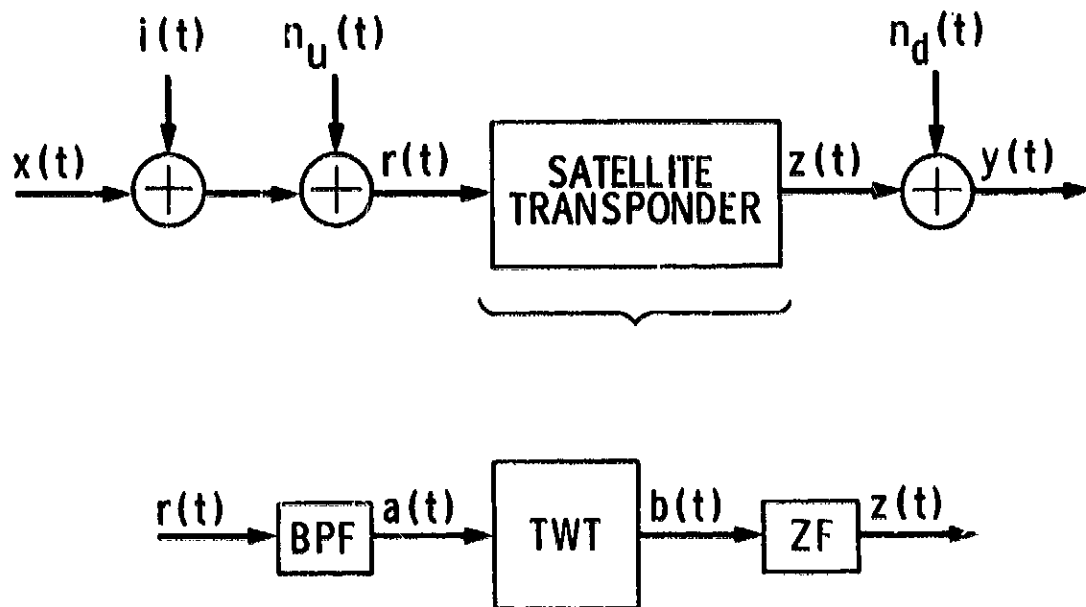
Figure 1.   Satellite Channel Model

5

the satellite transponder, and a downlink additive white Gaussian noise. The satellite transponder is modelled as a cascade of a bandpass filter and a travelling wave tube (TWT) amplifier followed by a zonal filter.

The input to the satellite transponder is given by

$$r(t) = x(t) + i(t) + n_u(t) \qquad\qquad (III.2.1)$$

where $x(t)$ is the "ideal" transmitted signal, $i(t)$ is the interference, and $n_u(t)$ is the uplink additive white Gaussian noise. Included in $i(t)$ is the possibility of various interference signals such as those due to adjacent channels, co-channel interferers, radar pulses, intentional jamming, multipath and intersymbol interference with the latter two being related to $x(t)$. We assume that $r(t)$ is passed through an ideal bandpass filter (BPF) that leaves the signal undistorted and limits the noise spectrum to that portion of the signal frequency band determined by the filter bandwidth. The BPF output is then

$$a(t) = x(t) + \tilde{n}_u(t) \qquad\qquad (III.2.2)$$

where $\tilde{n}_u(t)$ is the portion or component of the white Gaussian noise that is in the signal frequency band. Assuming a carrier frequency $f_0 = \omega_0/2\pi$, we have the narrowband signal representation

$$a(t) = R(t) \cos\left[\omega_0 t + \eta(t)\right] \qquad\qquad (III.2.3)$$

where the envelope $R(t)$ and phase $\eta(t)$ are "slowly varying" compared to the carrier oscillations.

We now consider a mathematical model for the TWT followed by the zonal filter. First let

$$A(t) = R(t) e^{j\left[\omega_0 t + \eta(t)\right]} \qquad\qquad (III.2.4)$$

be the complex signal representation of the narrowband signal $a(t)$ which enters the TWT. The TWT output complex signal $B(t)$ is assumed to be a memoryless complex function of the complex input signal given by

6

$$B(t) = F(A(t)) \tag{III.2.5}$$

Hence we assume the satellite's amplifier or TWT is an ideal memoryless device that introduces only amplitude and phase changes to the signal at its input. Defining

$$\phi(t) = \omega_0 t + \eta(t) \tag{III.2.6}$$

and suppressing the time dependence, we have the TWT output given by*

$$B = F(A)$$

$$= F(Re^{j\phi}) \tag{III.2.7}$$

which is periodic in ϕ. Hence B can be given a Fourier series representation in terms of harmonics of ϕ, namely

$$B = \sum_{n=-\infty}^{\infty} C_n(R) e^{jn\phi} \tag{III.2.8}$$

or reinstating the time parameter and substituting for $\phi(t)$ from (III.2.6),

$$B(t) = \sum_{n=-\infty}^{\infty} C_n(R(t)) e^{jn[\omega_0 t + \eta(t)]} \tag{III.2.9}$$

Here the Fourier series coefficients $\{C_n(R(t))\}$ depend only on $R(t)$ since the series expansion is performed over the variable ϕ with R held constant.

The complex signal $B(t)$ has the energy distribution sketched in Figure 2 where we make the usual "narrowband signal" assumption that $R(t)$ and $\eta(t)$ vary slow enough that the harmonic terms in the Fourier series have non-overlapping

---

*Occasionally in our discussion, we shall for notational convenience suppress the dependence of certain signals on the time parameter t.

SPECTRUM OF B(t)
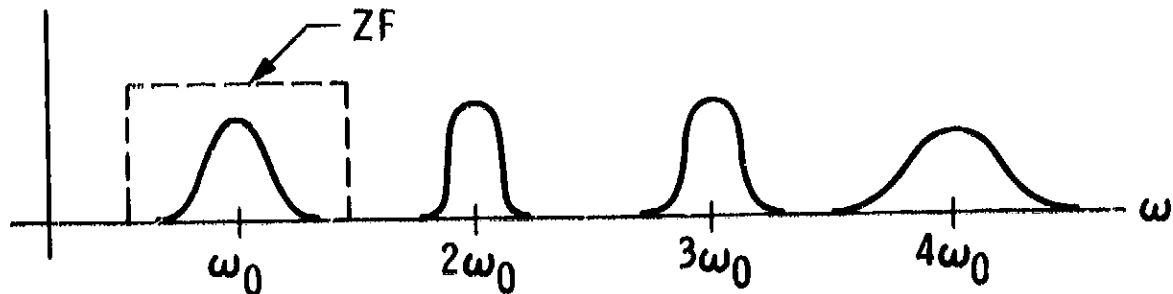
(NARROWBAND ASSUMPTION)
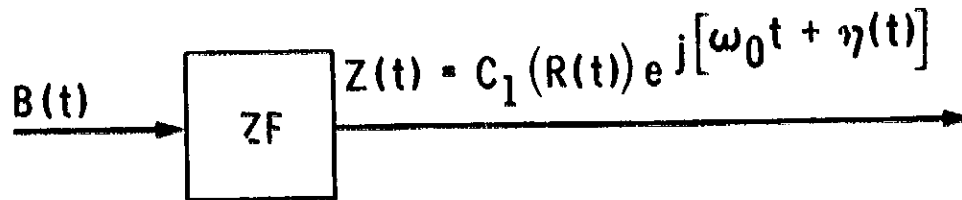
$$Z(t) = C_1(R(t)) e^{j\left[\omega_0 t + \eta(t)\right]}$$

Figure 2. Zonal Filter Output

spectra. The zonal filtering of B(t) results in the complex signal

$$Z(t) = C_1(R(t))e^{j[\omega_0 t + \eta(t)]} \tag{III.2.10}$$

where, since $C_1(R(t))$ is a complex coefficient, we can represent it in terms of a real envelope $f(R(t))$ and phase $g(R(t))$ as

$$C_1(R(t)) = f(R(t)) e^{jg(R(t))} \tag{III.2.11}$$

Thus the satellite output signal, in complex form, is

$$Z(t) = f(R(t)) e^{j[\omega_0 t + g(R(t)) + \eta(t)]} \tag{III.2.12}$$

8

which has the real part

$$z(t) = f(R(t)) \cos \left[\omega_0 t + g(R(t)) + n(t) \right] \qquad (III.2.13)$$

The envelope function, $f(\cdot)$, is commonly called the AM/AM function while the phase function, $g(\cdot)$, is called the AM/PM function. Special cases are:

Linear TWT: $\qquad\qquad\qquad\qquad\qquad f(R(t)) = \gamma\, R(t)$

$\qquad\qquad\qquad\qquad\qquad\qquad\qquad\qquad g(R(t)) = 0 \qquad$ (constant)

Hard Limiting TWT: $\qquad\qquad\qquad f(R(t)) = \gamma$

$\qquad\qquad\qquad\qquad\qquad\qquad\qquad\qquad g(R(t)) = 0 \qquad\qquad\qquad (III.2.14)$

Typically the AM/AM and AM/PM functions are given as measured TWT power and phase curves such as those shown in Figure 3.

A bandpass nonlinearity (BPNL) is any device that is characterized by AM/AM and AM/PM functions such as our model for the nonlinear satellite transponder. As shown in Figure 4 two BPNL's in cascade form another overall BPNL. Satellite systems that use soft limiters preceding the TWT amplifiers can thus be modeled as such.

Note that if the signal into the satellite has constant envelope

$$R(t) = R_0 \quad \text{(constant)} \qquad\qquad (III.2.15)$$

then the output signal

$$z(t) = f(R_0) \cos \left[\omega_0 t + g(R_0) + n(t) \right] \qquad\qquad (III.2.16)$$

is an undistorted amplification of the input signal with only a constant phase shift $g(R_0)$ which can be easily removed at the receiver. On the other hand, suppose the input to the satellite consists of a non-constant envelope signal such as the sum of two tones offset in frequency. Then, in the absence of noise

$$r(t) = \cos \left[(\omega_0 + \Delta\omega)t \right] + \cos \left[(\omega_0 - \Delta\omega)t + \phi_0 \right]$$

$$= R(t) \cos \left[\omega_0 t + n(t) \right] \qquad\qquad (III.2.17)$$

9

SINGLE-CARRIER OUTPUT PHASE, deg

OUTPUT PHASE

OUTPUT POWER

NORMALIZED SINGLE-CARRIER INPUT LEVEL, dB

NORMALIZED SINGLE-CARRIER OUTPUT LEVEL, dB
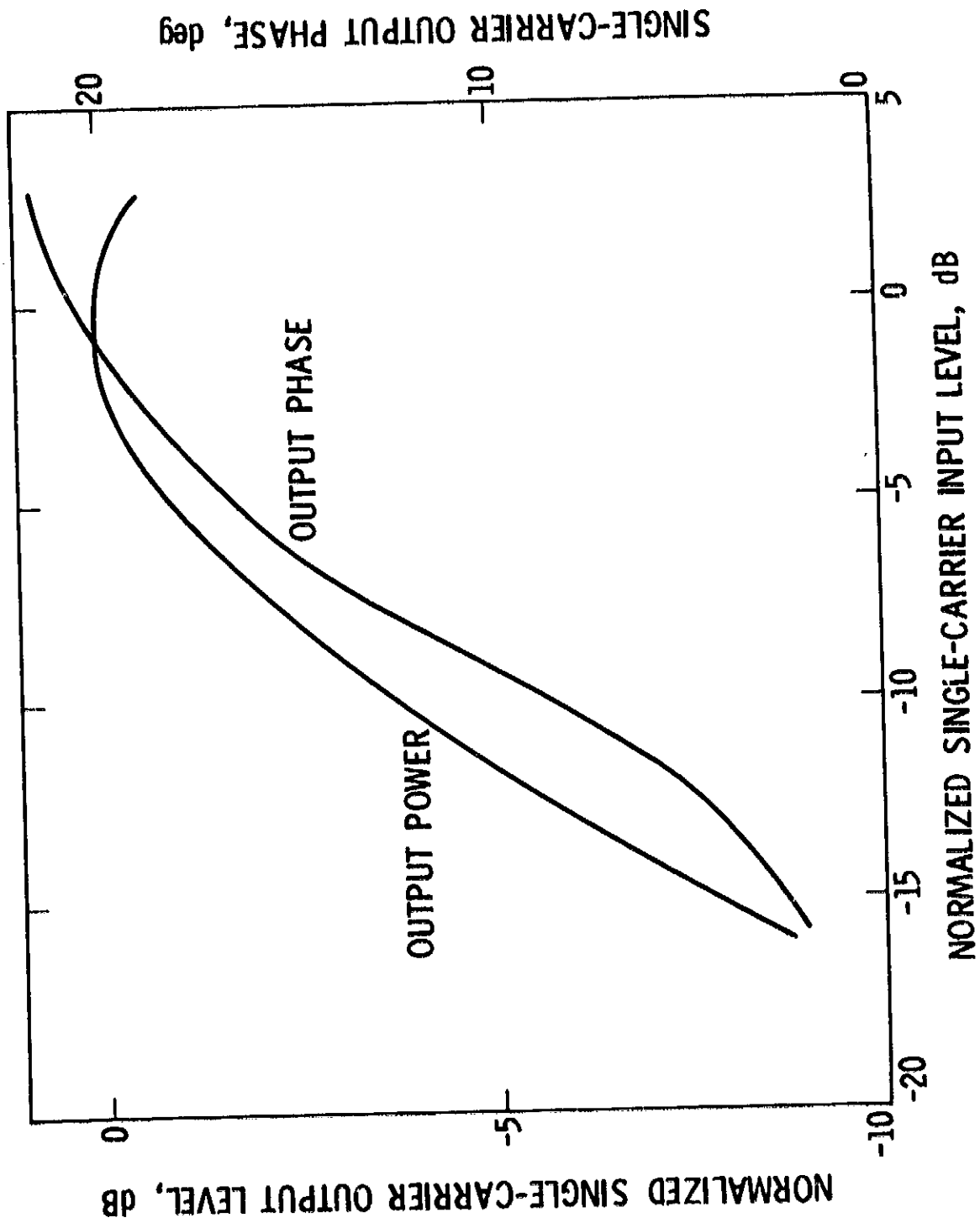
Figure 3. TWT Power and Phase Characteristics

10

$$x(t) \xrightarrow{\hspace{1cm}} \boxed{f_1(\cdot),\ g_1(\cdot)} \xrightarrow{\ y(t)\ } \boxed{f_2(\cdot),\ g_2(\cdot)} \xrightarrow{\ z(t)\ }$$

BPNL$_1$ BPNL$_2$

$$|||$$

$$x(t) \longrightarrow \boxed{\begin{array}{l} f(\cdot) = f_2(f_1(\cdot)) \\[4pt] g(\cdot) = g_2(f_1(\cdot)) + g_1(\cdot) \end{array}} \longrightarrow z(t)$$
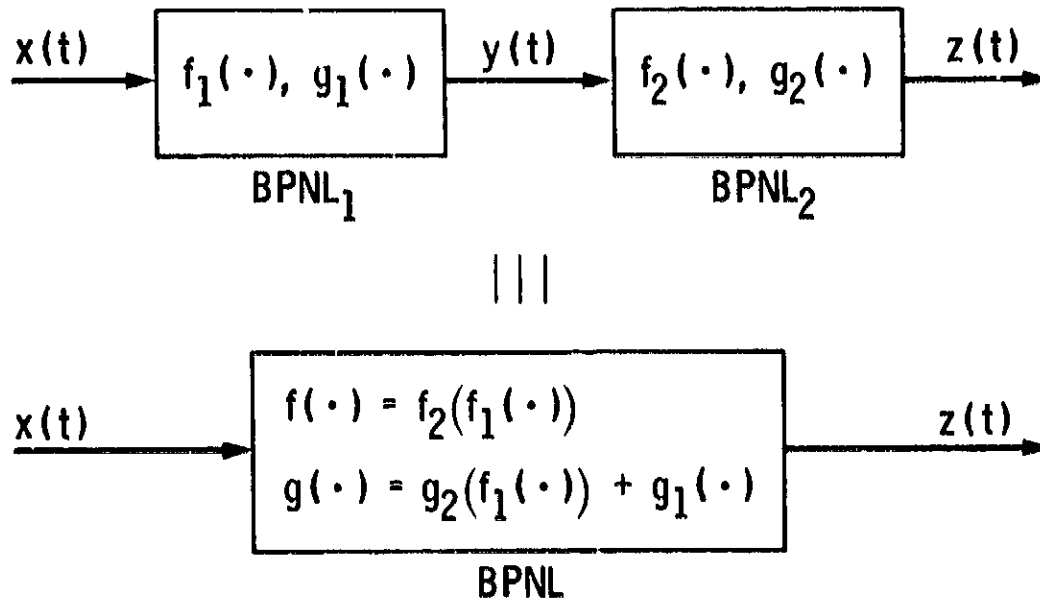
BPNL

$$x(t) = R(t) \cos\left[\omega_0 t + \eta(t)\right]$$

$$\downarrow$$

$$y(t) = f_1(R(t)) \cos\left[\omega_0 t + g_1(R(t)) + \eta(t)\right]$$

$$\downarrow$$

$$z(t) = f_2(f_1(R(t))) \cos\left[\omega_0 t + g_2(f_1(R(t))) + g_1(R(t)) + \eta(t)\right]$$

$$= f(R(t)) \cos\left[\omega_0 t + g(R(t)) + \eta(t)\right]$$

Figure 4. Cascade of Two BPNL

11

where

$$R(t) = \sqrt{(\cos \Lambda\omega t + \cos|\Lambda\omega t - \phi_0|)^2 + (\sin \Lambda\omega t - \sin |\Lambda\omega t - \phi_0|)^2}$$

(III.2.18)

and

$$\eta(t) = \tan^{-1} \frac{\sin [\Lambda\omega t - \phi_0] - \sin \Lambda\omega t}{\cos [\Lambda\omega t - \phi_0] + \cos \Lambda\omega t}$$
(III.2.19)

Figure 5 shows typical measured input and output signal spectra for a satellite with such a two-tone input.

In general with non-constant envelope signals into a satellite TWT, one has at the output intermodulation distortion of the original signal. The degree of distortion is a function of the AM/AM and AM/PM characteristics and the operating point of the TWT. With non-constant envelope signals into a satellite TWT, to minimize intermodulation distortions one generally "backs off" the TWT operating point to a region where the TWT acts approximately as a linear amplifier. This means that the satellite output power is not at its maximum capability and the downlink suffers a loss of potential channel capacity. Typically, to operate in a linear region, a TWT must be backed off 5 to 6 dB.

3.0   Some Additional Results for the Linear Channel

In Part II we described the linear channel which is modeled as an additive white Gaussian noise channel. Here, we briefly review the maximum-likelihood (ML) criterion for this channel and show how previously derived bit error bounds for the ML receiver can be modified when this receiver is used on channels which are not matched to it. In such mismatch situations, the receiver metric is not ML for the actual channel at hand.

Suppose the data sequence u results in a transmitted waveform $x(t;\underline{u})$. Then the output of the channel has the form

$$y(t) = x(t;\underline{u}) + n(t)$$
(III.3.1)

12

Two tones are transmitted to the satellite as shown:
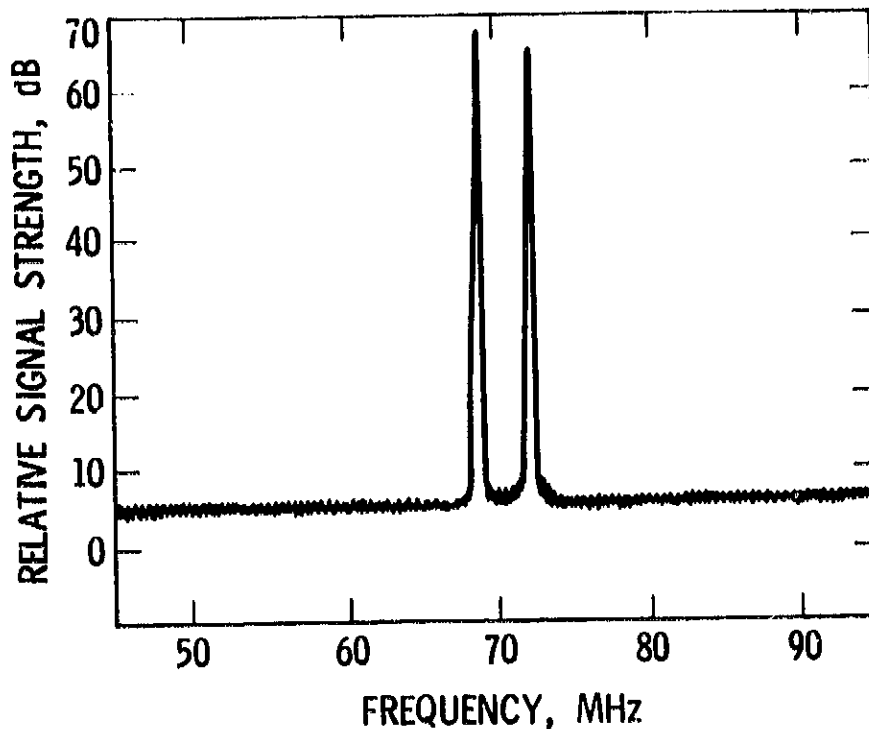
The following signal is received at Earth stations, showing how intermodulation has occurred between the two tones:
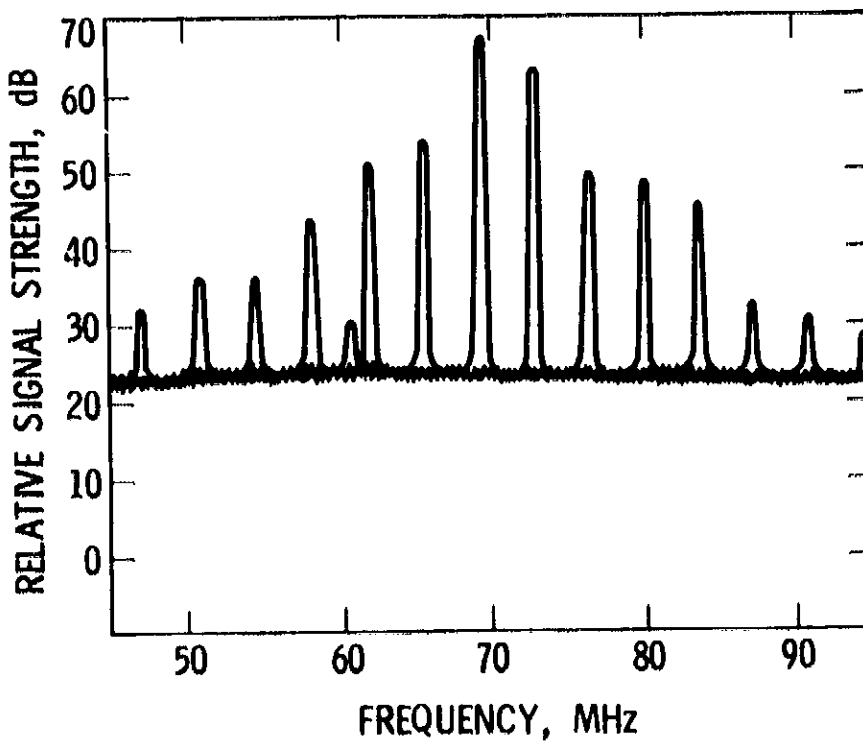
Figure 5.   Intermodulation Measurements

13

where $n(t)$ is a white Gaussian noise process with double-sided spectral density $N_0/2$. The ML receiver decides that the sequence $\hat{u}$ was transmitted where $\hat{u}$ yields the maximum value of the total metric

$$m(y;\underline{u}) = \int_{-\infty}^{\infty} y(t)x(t;\underline{u})dt - \frac{1}{2}\int_{-\infty}^{\infty} x^2(t;\underline{u})dt \qquad (III.3.2)$$

over all possible data sequences $\tilde{\underline{u}}$.

In many cases of interest, the signal during any T-second symbol interval is characterized by a "state" and a data symbol. That is,

$$x(t;\underline{u}) = x(t;\tilde{s}_n,\tilde{u}_n); \quad nT \leq t \leq (n+1)T$$

$$\text{for all } n \qquad (III.3.3)$$

where $\tilde{u}_n$ is the $\underline{nth}$ data symbol and $\tilde{s}_n$ is the "state" at the beginning of the $\underline{nth}$ T-second interval. Then, the above total metric can be written in the form

$$\sum_{n=-\infty}^{\infty} m(\underline{y}_n;s_n,u_n)$$

where

$$m(\underline{y}_n;s_n,u_n) = \int_{nT}^{(n+1)T} y(t)x(t;s_n,u_n)dt - \frac{1}{2}\int_{-\infty}^{\infty} x^2(t;s_n,u_n)dt$$

$$(III.3.4)$$

Here $\underline{y}_n$ denotes the statistic that represents $y(t)$ in the $\underline{nth}$ transmission interval.

In Part II, we presented many examples of ML receivers for various modulations. In all cases, the key to deriving general symbol error probability bounds for these receivers was to first derive pair-wise error bounds. Suppose, for

14

example that $\underline{u}$ is the actual transmitted data sequence. Then, the probability $Pr(\underline{u} > \underline{\hat{u}})$ that some other sequence $\underline{\hat{u}}$ has larger total metric was shown to have the upper bound

$$Pr(\underline{u} > \underline{\hat{u}}) \leq \prod_{n=-\infty}^{\infty} D((\hat{s}_n, \hat{u}_n), (s_n, u_n)) \qquad (III.3.5)$$

where

$$D((\hat{s}_n, \hat{u}_n), (s_n, u_n)) = \exp\left\{-\frac{1}{4N_0} \int_{nT}^{(n+1)T} [x(t; s_n, u_n) - x(t; \hat{s}_n, \hat{u}_n)]^2 dt\right\}$$

$$(III.3.6)$$

Having a bound on the pair-wise error probability that is a product of terms involving only the data symbols and the corresponding states was shown to be necessary in order to use the transfer function bounds discussed in Appendix A of Part IV.

3.1 Pair-wise Error Bound - Mismatched Receiver

In many practical situations the channel may have a different form than that assumed by the receiver. That is, the receiver may use a metric $m(y_n; s_n, u_n)$ which is not the ML metric for the actual channel. The channel, for example, may have multipath or cochannel interference while the receiver assumes the channel is the ideal additive white Gaussian noise channel and uses the decision rule based on this assumption.

To evaluate a symbol error bound for this "mismatched" case, we again consider the pair-wise error probability between two data sequences $\underline{u}$ and $\underline{\hat{u}}$. Consider the Chernoff bound,

$$Pr(\underline{u} > \underline{\hat{u}}) = Pr\left\{\sum_{n=-\infty}^{\infty} m(y_n; s_n, u_n) < \sum_{n=-\infty}^{\infty} m(y_n; \hat{s}_n, \hat{u}_n) \,\Big|\, \underline{u}\right\}$$

$$= Pr\left\{\sum_{n=-\infty}^{\infty} [m(y_n; \hat{s}_n, \hat{u}_n) - m(y_n; s_n, u_n)] > 0 \,\Big|\, \underline{u}\right\}$$

15

$$\leq E\left\{\exp\left\{\lambda\sum_{n=-\infty}^{\infty}[m(y_n;\hat{s}_n,\hat{u}_n) - m(y_n;s_n,u_n)]\right\}\right\}$$

$$= E\left\{\prod_{n=-\infty}^{\infty}\exp\left\{\lambda[m(y_n;\hat{s}_n,\hat{u}_n) - m(y_n;s_n,u_n)]\right\}\right\} \qquad \text{(III.3.7)}$$

where λ is any non-negative number referred to as the Chernoff bound parameter and the expectation is over the channel random disturbances. Generally, we assume these disturbances are independent over each non-overlapping T-second time interval so that

$$\Pr(\underline{u}\to\hat{\underline{u}}) \leq \prod_{n=-\infty}^{\infty} E\left\{\exp\left\{\lambda[m(\underline{y}_n;\hat{s}_n,\hat{u}_n) - m(\underline{y}_n;s_n,u_n)]\right\}\right\}$$

$$= \prod_{n=-\infty}^{\infty} D_\lambda((\hat{s}_n,\hat{u}_n),(s_n,u_n)) \qquad \text{(III.3.8)}$$

where

$$D_\lambda((\hat{s}_n,\hat{u}_n),(s_n,u_n)) = E\left\{\exp\left\{\lambda[m(\underline{y}_n;\hat{s}_n,\hat{u}_n) - m(\underline{y}_n;s_n,u_n)]\right\}\right\} \qquad \text{(III.3.9)}$$

When, in fact, the channel is the ideal additive white Gaussian noise channel, by minimizing (III.3.8) with respect to λ, we obtain the previous result, namely, (III.3.6).

The symbol error probability can be found in this mismatched case by again using the transfer function bound approach described in Appendix A of Part IV. Also the final bound can be further reduced by a factor of one-half as discussed in Appendix B of Part IV.

As an example suppose the actual channel had both additive interference i(t) as well as additive white Gaussian noise n(t). Then, the channel output is

$$y(t) = x(t;u) + v(t) \qquad \text{(III.3.10)}$$

16

where

$$v(t) = I(t) + n(t) \qquad (III.3.11)$$

and u_n is still the transmitted data sequence. Suppose that despite the presence of $I(t)$, the receiver uses the ML metric for the ideal additive white Gaussian noise channel namely (III.3.4). Then, for $y(t)$ in (III.3.10), we have

$$m(y_n; \hat{s}_n, \hat{u}_n) = \int_{nT}^{(n+1)T} y(t)x(t; \hat{s}_n, \hat{u}_n)dt - \frac{1}{2}\int_{nT}^{(n+1)T} x^2(t; \hat{s}_n, \hat{u}_n)dt$$

$$= \int_{nT}^{(n+1)T} x(t; s_n, u_n)x(t; \hat{s}_n, \hat{u}_n)dt$$

$$+ \int_{nT}^{(n+1)T} v(t)x(t; \hat{s}_n, \hat{u}_n)dt - \frac{1}{2}\int_{nT}^{(n+1)T} x^2(t; \hat{s}_n, \hat{u}_n)dt$$

$$(III.3.12)$$

and for constant envelope signals

$$m(y_n; \hat{s}_n, \hat{u}_n) - m(y_n; s_n, u_n) = \int_{nT}^{(n+1)T} x(t; s_n, u_n)[x(t; \hat{s}_n, \hat{u}_n) - x(t; s_n, u_n)]dt$$

$$+ \int_{nT}^{(n+1)T} v(t)[x(t; \hat{s}_n, \hat{u}_n) - x(t; s_n, u_n)]dt$$

$$(III.3.13)$$

17

Next we need to evaluate

$$D_\lambda((\hat{s}_n, \hat{u}_n), (s_n, u_n)) = \exp\left\{ \lambda \int_{nT}^{(n+1)T} x(t; s_n, u_n)[x(t; \hat{s}_n, \hat{u}_n) - x(t; s_n, u_n)]dt \right\}$$

$$\times E\left\{ \exp\left\{ \lambda \int_{nT}^{(n+1)T} v(t)[x(t; \hat{s}_n, \hat{u}_n) - x(t; s_n, u_n)]dt \right\} \right\}$$

$$(III.3.14)$$

where, recalling the definition of $v(t)$ in (III.3.11), $E\{\cdot\}$ is the expectation over the uplink noise $n(t)$ and interference $i(t)$. This expectation can be evaluated by first performing the expectation over the noise process which is easily done since

$$\int_{nT}^{(n+1)T} n(t)[x(t; \hat{s}_n, \hat{u}_n) - x(t; s_n, u_n)]dt$$

is a Gaussian random variable. The expectation over the uplink interference term

$$\int_{nT}^{(n+1)T} i(t)[x(t; \hat{s}_n, \hat{u}_n) - x(t; s_n, u_n)]dt$$

can either be performed directly for a given interference model or by using a computational technique based on moments [42] provided that moments of this term can be computed. Once these two components of the expectation are evaluated, then multiplying them together gives the expectation required in (III.3.14). Finally, substituting (III.3.14) into (III.3.5) gives the pair-wise error bound $Pr(u \cdot \hat{u})$ for this particular mismatched case which can then be used to obtain the bit error probability transfer function bounds as per the approach discussed in Appendix A of Part IV.

As an example of the application of the above discussion, we now evaluate the general Chernoff bound parameter given in (III.3.14) for the case of BPSK modulation with additive white Gaussian noise and interference. The signal has the form*

$$x(t;s_n,u_n) = u_n \sqrt{2S} \cos \omega_0 t; \quad nT \leq t \leq (n+1)T \qquad (III.3.15)$$

where u_n is the independent identically distributed binary data sequence with

$$Pr\{u_n = 1\} = Pr\{u_n = -1\} = \frac{1}{2} \qquad (III.3.16)$$

Thus, the integral in the first exponential of (III.3.14) is evaluated as

$$\int_{nT}^{(n+1)T} x(t;s_n,u_n)[x(t;\hat{s}_n,\hat{u}_n) - x(t;s_n,u_n)]dt$$

$$= \begin{cases} 0; & \hat{u}_n = u_n \\ -2E_b; & \hat{u}_n \neq u_n \end{cases} \qquad (III.3.17)$$

where

$$E_b = ST \qquad (III.3.18)$$

is the bit energy. Similarly, the integral involving the noise in the second exponential of (III.3.14) becomes

$$\int_{nT}^{(n+1)T} n(t)[x(t;s_n,\hat{u}_n) - x(t;s_n,u_n)]dt$$

---

*Note that for this form of modulation, there is no dependence on the state s_n.

19

$$= \begin{cases} 0 \; ; & \hat{u}_n = u_n \\ -\sqrt{2E_b N_0} \, u_n \, n_{n,c} \; ; & \hat{u}_n \neq u_n \end{cases} \qquad (III.3.19)$$

where $n_{n,c}$ is a zero mean, unit variance Gaussian random variable. Finally, when $\hat{u}_n \neq u_n$, the interference term becomes

$$\int_{nT}^{(n+1)T} i(t)[x(t;\hat{s}_n,\hat{u}_n) - x(t;s_n,u_n)]dt$$

$$= -2\sqrt{2S} \, u_n \int_{nT}^{(n+1)T} i(t) \cos \omega_0 t \, dt \qquad (III.3.20)$$

We assume the random variable

$$i_n \triangleq \frac{1}{T} \int_{nT}^{(n+1)T} i(t) \cos \omega_0 t \, dt \qquad (III.3.21)$$

has a symmetric probability density function with moment generating function

$$\Phi(\omega) = E\left\{e^{\omega i_n}\right\} \qquad (III.3.22)$$

which is an even function of ω.

Proceeding now to evaluate the expectations required in (III.3.14) using (III.3.19) and (III.3.20) we obtain the following results. Since for $\hat{u}_n = u_n$ both integrals evaluate to zero, then the expectation of the exponential of these quantities clearly evaluates to unity. On the other hand, for $\hat{u}_n \neq u_n$, we have

20

$$E\left\{\exp\left\{\lambda\int_{nT}^{(n+1)T} n(t)[x(t;\hat{s}_n,\hat{u}_n) - x(t;s_n,u_n)]dt\right\}\right\}$$

$$= E\left\{\exp\left\{-\lambda\sqrt{2E_bN_0}\, u_n\, n_{n,c}\right\}\right\}$$

$$= \exp\left\{\lambda^2 E_b N_0\right\} \tag{III.3.23}$$

and

$$E\left\{\exp\left\{\lambda\int_{nT}^{(n+1)T} i(t)[x(t;\hat{s}_n,\hat{u}_n) - x(t;s_n,u_n)]dt\right\}\right\}$$

$$= E\left\{\exp\left\{-2\lambda\sqrt{2S}\,T\, u_n\, i_n\right\}\right\}$$

$$= \phi(2\lambda\sqrt{2S}\,T) \tag{III.3.24}$$

respectively. Thus, for this case, (III.3.14) has the simple form

$$D_\lambda((\hat{s}_n,\hat{u}_n),(s_n,u_n)) = \begin{cases} 1; & \hat{u}_n = u_n \\ \\ \exp(-2\lambda E_b + \lambda^2 E_b N_0)\,\phi(2\lambda\sqrt{2S}\,T); & \hat{u}_n \neq u_n \end{cases}$$

$$\tag{III.3.25}$$

The moment generating function of the interference term in (III.3.24) can be evaluated based on mathematical models of the interference signal. For example, pulses due to many radar sources might result in the model

$$i_n = \sum_{i=1}^{N_T} z_i \tag{III.3.26}$$

21

where $\{z_i\}$ are i.i.d. random variables uniformly distributed in the interval $[-1,1]$ while N_T is a Poisson random variable with probability density function

$$\Pr\{N_T = k\} = \frac{(\beta T)^k}{k!}\, e^{-\beta T}; \quad k = 0,1,2,\ldots$$

(III.3.27)

where βT represents the average number of pulses occurring in the bit interval T. For this case,

$$\Phi(\omega) = E\left\{e^{\omega n}\right\}$$

$$= E\left\{\prod_{i=1}^{N_T} e^{\omega z_i}\right\}$$

$$= E\left\{E\left\{\prod_{i=1}^{N_T} e^{\omega z_i}\,\Big|\,N_T\right\}\right\}$$

$$= E\left\{\prod_{i=1}^{N_T} E\{e^{\omega z_i}\}\right\}$$

$$= E\left\{\left(\frac{\sinh \omega}{\omega}\right)^{N_T}\right\}$$

$$= \exp\left\{\beta T\left[\frac{\sinh \omega}{\omega} - 1\right]\right\}$$

(III.3.28)

Evaluating (III.3.28) at $\omega = 2\lambda\sqrt{2S}$ and further letting $\lambda_0 = \lambda N_0$, we get the normalized form of (III.3.25) as

$$D_{\lambda_0}((\hat{s}_n, \hat{u}_n), (s_n, v_n)) = \begin{cases} 1 \; ; \; \hat{u}_n = u_n \\ \\ \exp\left\{-2\lambda_0 E_b/N_0 + \lambda_0^2 E_b/N_0 + \beta T\left[\dfrac{\sinh 2\sqrt{2}\,\lambda_0\left(\dfrac{E_b}{N_0}\right)\left(\dfrac{L}{\sqrt{S}}\right)}{2\sqrt{2}\,\lambda_0\left(\dfrac{E_b}{N_0}\right)\left(\dfrac{L}{\sqrt{S}}\right)} - 1\right]\right\} \; ; \\ \hat{u}_n \neq u_n \end{cases}$$

$$(\text{III}.3.29)$$

which in general, must be minimized with respect to λ_0. If the interference-to-signal power ratio is small, i.e., $L/\sqrt{S} \ll 1$, then we can approximate the sinh function by the first two terms of its Maclaurin series expansion which simplifies (III.3.29) to

$$D_{\lambda_0}((\hat{s}_n, \hat{u}_n), (s_n, u_n)) = \begin{cases} 1 \; ; \; \hat{u}_n = u_n \\ \\ \exp\left\{-2\lambda_0 E_b/N_0 + \lambda_0^2 E_b/N_0 + 4\lambda_0^2 (E_b/N_0)^2 (I/S)\right\} \; ; \; \hat{u}_n \neq u_n \end{cases}$$

$$(\text{III}.3.30)$$

where

$$I \stackrel{\Delta}{=} \phi''(0) = \beta T L^2/3 \qquad\qquad (\text{III}.3.31)$$

is the total interference power of I_n. Minimizing (III.3.30) over λ_0 results in

$$D = \min_{\lambda_0} D_{\lambda_0}((\hat{s}_n, \hat{u}_n), (s_n, u_n)) = \begin{cases} 1 \; ; \; \hat{u}_n = u_n \\ \\ \exp\left\{-\dfrac{E_b/N_0}{1 + 4(I/S)(E_b/N_0)}\right\} \; ; \; \hat{u}_n \neq u_n \end{cases}$$

$$(\text{III}.3.32)$$

Figure 6 is an illustration of D versus E_b/N_0 for various values of I/S.

Another approach to evaluating the moment generating function of I_n is to approximate it using moments of the random variable I_n. Intersymbol Interference and cochannel interference where I_n is a sum of independent random variables are cases where this approach is useful.

4.0   Nonlinear Channel

We now consider the satellite channel of Figure 1. During the nth transmission interval, $nT \leq t \leq (n+1)T$, the uplink signal is $x(t;s_n,u_n)$ resulting in the satellite input signal of the form

$$r(t) = x(t;s_n,u_n) + I(t) + n_u(t) \qquad (III.4.1)$$

After passing through the satellite bandpass filter this signal becomes

$$a(t) = x(t;s_n,u_n) + v(t) \qquad (III.4.2)$$

where we have assumed that the signal passes undistorted and $v(t)$ is the filtered uplink interference plus noise.

Since $a(t)$ is a narrowband signal, we can represent it as in (III.2.3) where the envelope $R(t)$ and phase $u(t)$ depend on both the uplink signal and the filtered uplink interference plus noise term $v(t)$. Using the first-order model for the satellite transponder, the satellite downlink signal is given by $z(t)$ of (III.2.13). For the nth interval, $nT \leq t \leq (n+1)T$, $z(t)$ clearly depends on the nth data symbol u_n and the nth state s_n as well as the bandpass filtered uplink interference plus noise terms.

The downlink channel is assumed to be an ideal additive white Gaussian noise channel resulting in the signal

$$y(t) = z(t) + n_d(t) \qquad (III.4.3)$$

at the input to the receiver. We now examine the evaluation of performance for two types of receivers.
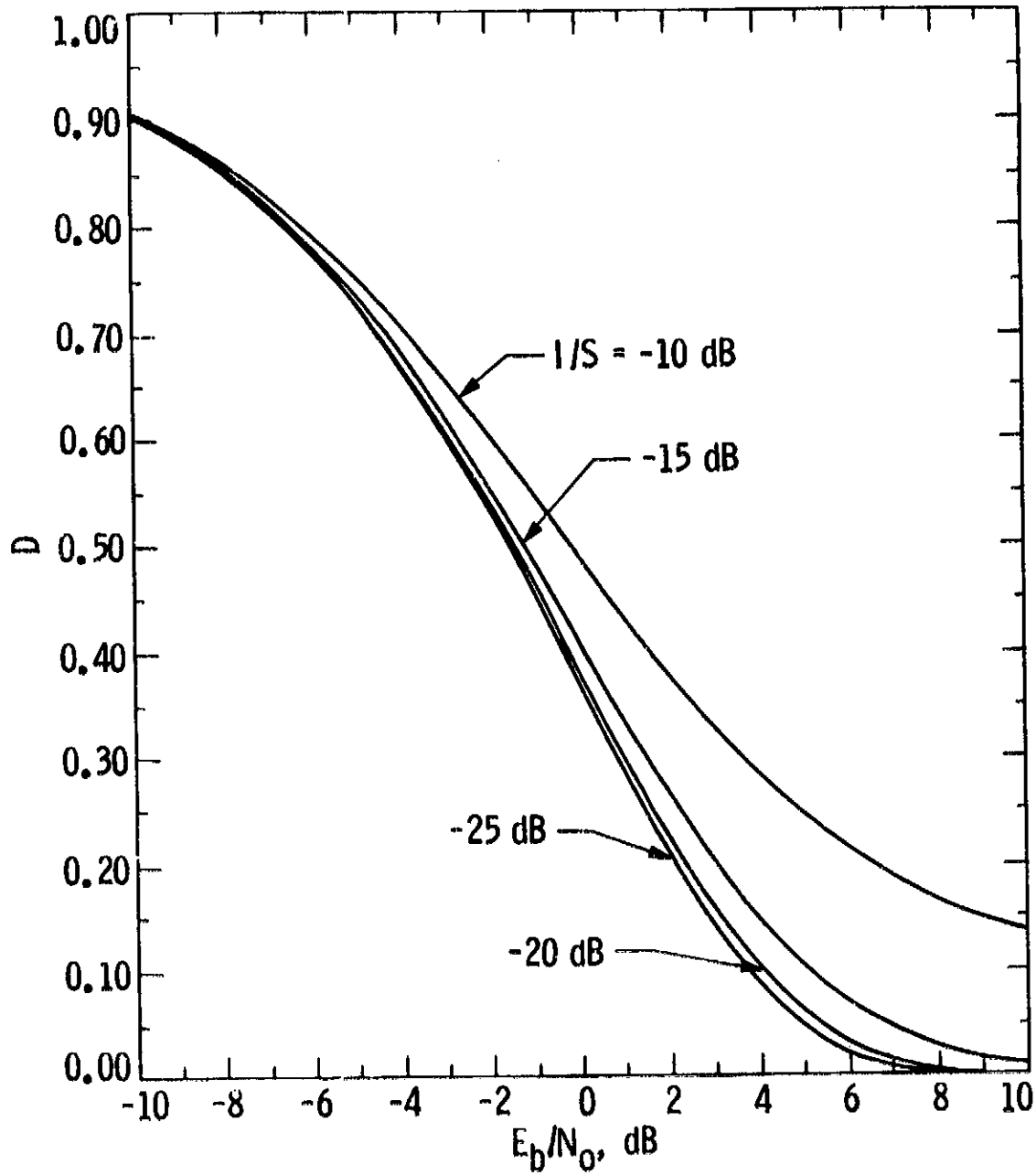
Figure 6. Chernoff Bound D versus Bit Energy-to-Noise Ratio E_b/N_0 in dB for Various Values of Interference-to-Signal Power Ratio I/S in dB

4.1 Mismatched Receiver

Most receiver designs are based on the ideal additive white Gaussian noise channel. Such receivers, however, are mismatched to the satellite channel since they no longer form a true maximum-likelihood (ML) decision rule. Here we assume the mismatched receiver based on the ML decision rule for the ideal additive white Gaussian noise channel with symbol metric as in (III.3.4). Again when $x(t; \overset{\vee}{s}_n, \overset{\vee}{u}_n)$ is a constant envelope signal we have, analogous to (III.3.13),

$$m(\underline{y}_n; \hat{s}_n, \hat{u}_n) - m(\underline{y}_n; s_n, u_n)$$

$$= \int_{nT}^{(n+1)T} z(t)[x(t; \hat{s}_n, \hat{u}_n) - x(t; s_n, u_n)]dt$$

$$+ \int_{nT}^{(n+1)T} n_d(t)[x(t; \hat{s}_n, \hat{u}_n) - x(t; s_n, u_n)]dt$$

$$(III.4.4)$$

The term

$$N_d = \int_{nT}^{(n+1)T} n_d(t)[x(t; \hat{s}_n, \hat{u}_n) - x(t; s_n, u_n)]dt$$

$$(III.4.5)$$

is a zero mean Gaussian random variable with variance

$$\sigma_d^2 = \frac{N_{0d}}{2} \int_{nT}^{(n+1)T} [x(t; \hat{s}_n, \hat{u}_n) - x(t; s_n, u_n)]^2 dt$$

$$(III.4.6)$$

where N_{0d} is the downlink noise spectral density in watts/Hz. Since

$$E\left\{e^{\lambda N_d}\right\} = \exp\left\{\frac{1}{2}\lambda^2 \sigma_d^2\right\} \qquad (III.4.7)$$

we have from (III.3.9) that

$$D_\lambda\left((s_n, u_n), (\hat{s}_n, \hat{u}_n)\right) = E\left\{\exp\{\lambda[m(y_n; \hat{s}_n, \hat{u}_n) - m(y_n; s_n, u_n)]\}\right\}$$

$$= \exp\left\{\frac{N_{0d}}{4}\lambda^2 \int_{nT}^{(n+1)T} [x(t; \hat{s}_n, \hat{u}_n) - x(t; s_n, u_n)]^2 dt\right\}$$

$$\times E\left\{\exp\{\lambda \int_{nT}^{(n+1)T} z(t)[x(t; \hat{s}_n, \hat{u}_n) - x(t; s_n, u_n)]dt\}\right\}$$

$$(III.4.8)$$

where $E\{\cdot\}$ is the expected value over the uplink filtered interference plus noise, $v(t)$. The numerical evaluation of this expectation is the key to evaluating transfer function bit error bounds for all the various satellite communication systems.

Because of the memory associated with the integration over the nth data symbol interval $(nT, (n+1)T)$, the above evaluation is quite difficult to accomplish unless one is willing to make some simplifying assumptions. One such simplification is to assume that the satellite transponder BPF is ideal in that it limits the satellite input signal $r(t)$ to the signal space generated by the pair of quadrature basis functions

$$\phi_c(t) = \sqrt{\frac{2}{T}} \cos \omega_0 t$$

$$\phi_s(t) = -\sqrt{\frac{2}{T}} \sin \omega_0 t; \quad 0 \le t \le T \qquad (III.4.9)$$

27

Equivalently, the filtered version of $r(t)$ has the form

$$a(t) = x(t; s_n, u_n) + \tilde{v}(t)$$

$$= r_{n,c} \phi_{n,c}(t) + r_{n,s} \phi_{n,s}(t); \quad nT \leq t \leq (n+1)T$$

(III.4.10)

which has only two degrees of freedom characterized in each T-second interval by the pair of orthonormal functions

$$\phi_{n,c}(t) = \phi_c(t-nT)$$

$$\phi_{n,s}(t) = \phi_s(t-nT); \quad nT \leq t \leq (n+1)T$$

(III.4.11)

and coefficients

$$r_{n,c} = \int_{nT}^{(n+1)T} r(t)\phi_{n,c}(t)dt = x_{n,c} + N_{n,c} + i_{n,c}$$

$$r_{n,s} = \int_{nT}^{(n+1)T} r(t)\phi_{n,s}(t)dt = x_{n,s} + N_{n,s} + i_{n,s}$$

(III.4.12)

which are the projections of $r(t)$ on these basis coordinates.

In (III.4.12), $(x_{n,c}, x_{n,s})$ are the quadrature signal components, $(N_{n,c}, N_{n,s})$ are the quadrature uplink noise components which are independent with zero mean and variance $\sigma_u^2 = N_{0u}/2$, and $(i_{n,c}, i_{n,s})$ are the quadrature components of the uplink interference.

With the above approximate model, the uplink signal envelope is

$$R = \sqrt{r_{n,c}^2 + r_{n,s}^2} \qquad \text{(III.4.13)}$$

and its phase is

$$\eta = \tan^{-1}\left[\frac{r_{n,s}}{r_{n,c}}\right] \qquad \text{(III.4.14)}$$

The corresponding satellite output signal of (III.2.13) then has the form

$$z(t) = \sqrt{\frac{T}{2}} f(R) \cos (g(R) + \eta)\phi_{n,c}(t)$$

$$+ \sqrt{\frac{T}{2}} f(R) \sin (g(R) + \eta)\phi_{n,s}(t) \qquad \text{(III.4.15)}$$

which is a function of the uplink signal, the noise components $(N_{n,c}, N_{n,s})$ and the interference components $(i_{n,c}, i_{n,s})$. Thus, the evaluation of*

$$E\left\{\exp\left\{\lambda \int_{nT}^{(n+1)T} z(t)[x(t;\hat{s}_n,\hat{u}_n) - x(t;s_n,u_n)]dt\right\}\right\}$$

$$= E\left\{\exp\left\{\lambda\sqrt{\frac{T}{2}} f(R)[(\hat{x}_{n,c} - x_{n,c}) \cos (g(R) + \eta - \bar{g})\right.\right.$$

$$\left.\left. + (\hat{x}_{n,s} - x_{n,s}) \sin (g(R) + \eta - \bar{g})]\right\}\right\} \qquad \text{(III.4.16)}$$

involves the expectation over the two independent Gaussian random variables and the two interference random variables. Since $N_{n,c}$ and $N_{n,s}$ are independent of

*We assume that a phase-locked loop tracks the long time average of the satellite output signal and $\bar{g}$ is the phase of the loop's reference signal so produced.

each other, the expectation over these uplink noise components can be approximated using the Gauss-Quadrature rules [43]. The difficult part of the above evaluation is the expectation over the typically correlated interference random variables $i_{n,c}$ and $i_{n,s}$.

As an illustration of the evaluation of (III.4.8) using (III.4.16), we consider again the BPSK example of the previous section where $x(t;s_n,u_n)$ is characterized by (III.3.15) together with (III.3.16). Here the coefficients of (III.4.12) become

$$r_{n,c} = u_n \sqrt{E_b} + N_{n,c} + i_{n,c}$$

$$r_{n,s} = N_{n,s} + i_{n,s} \qquad\qquad (III.4.17)$$

Noting that for our simplified model

$$\int_{nT}^{(n+1)T} [x(t;\hat{s}_n,\hat{u}_n) - x(t;s_n,u_n)]^2 dt = (\hat{x}_{n,c} - x_{n,c})^2 + (\hat{x}_{n,s} - x_{n,s})^2$$

$$= \begin{cases} 0; & \hat{u}_n = u_n \\ 4E_b; & \hat{u}_n \neq u_n \end{cases} \qquad (III.4.18)$$

and

$$f(R)\left[(\hat{x}_{n,c} - x_{n,c}) \cos (g(R) + \eta - \bar{g}) + (\hat{x}_{n,s} - x_{n,s}) \sin (g(R) + \eta - \bar{g})\right]$$

$$= \begin{cases} 0; \quad \hat{u}_n = u_n \\ \\ - 2u_n \sqrt{E_b} \; f\left(\sqrt{(u_n \sqrt{E_b} + N_{n,c} + i_{n,c})^2 + (N_{n,s} + i_{n,s})^2}\right) \\ \\ \times \cos \left(g\left(\sqrt{(u_n \sqrt{E_b} + N_{n,c} + i_{n,c})^2 + (N_{n,s} + i_{n,s})^2}\right) + \tan^{-1}\left[\dfrac{N_{n,s} + i_{n,s}}{u_n \sqrt{E_b} + N_{n,c} + i_{n,c}}\right] - \bar{g}\right); \\ \\ \hat{u}_n \neq u_n \end{cases}$$

$$(III.4.19)$$

then, performing the average over $N_{n,c}$ and $N_{n,s}$ given

$$D_\lambda\left((\hat{s}_n,\hat{u}_n),(s_n,u_n)\right) = \begin{cases} 1; & \hat{u}_n = u_n \\ \\ \exp\{\lambda^2 E_b N_{0d}\}E\left[\sum_{i=1}^{N_\nu}\sum_{j=1}^{N_\nu} w_i w_j \exp\left|-2\lambda u_n\sqrt{E_b}\right| \right. \\ \\ \left. \times \xi (u_n,i_{n,c},i_{n,s},N_i,N_j)\}\right]; & \hat{u}_n \neq u_n \end{cases}$$

(III.4.20)

where

$$\xi(u_n,i_{n,c},i_{n,s},N_i,N_j) \triangleq \sqrt{\tfrac{T}{2}}\, f\left(\sqrt{(u_n\sqrt{E_b} + N_i + i_{n,c})^2 + (N_j + i_{n,s})^2}\right)$$

$$\times \cos\left(g\left(\sqrt{(u_n\sqrt{E_b} + N_i + i_{n,c})^2 + (N_j + i_{n,s})^2}\right)\right.$$

$$\left. + \tan^{-1}\left[\frac{N_j + i_{n,s}}{u_n\sqrt{E_b} + N_i + i_{n,c}}\right] - \bar{g}\right)$$

(III.4.21)

In (III.4.20), the expectation is now only over $i_{n,c}$ and $i_{n,s}$ while in (III.4.21), $\{N_i\}$ are the N_ν mass points for the Gauss-Hermite quadrature formula and $\{w_i\}$ are the corresponding N_ν weights. Appendix B of [43] tabulates sets of normalized mass points $\{N_i'\}$ and normalized weights $\{w_i'\}$ for values of N_ν from 1 to 20. To relate the normalized mass points and weights to the unnormalized ones needed in (III.4.21) we use the relations

31

$$N_i' = N_i/\sqrt{2}\sigma_n = N_i/\sqrt{N_{0u}}$$

$$w_i' = \sqrt{\pi}w_i \; ; \; i=1,2,\ldots, N_\nu \qquad (III.4.22)$$

To evaluate (III.4.20) any further, in particular, to perform the minimization over λ, we must specify particular AM/AM and AM/PM characteristics $f(R)$ and $g(R)$, respectively, and an interference model from which the random variables $i_{n,c}$ and $i_{n,s}$ can be statistically modeled. The simplest nonlinear model is that of a hard-limiting satellite repeater as characterized in (III.2.14). For this case, (III.4.21) simplifies to

$$\xi(u_n, i_{n,c}, i_{n,s}, N_i, N_j) = \sqrt{\frac{\pi}{2}}\,\gamma \cdot \frac{u_n\sqrt{E_b} + N_i + i_{n,c}}{\sqrt{(u_n\sqrt{E_b} + N_i + i_{n,c})^2 + (N_j + i_{n,s})^2}}$$

$$(III.4.23)$$

If furthermore, we assume that $i(t) = 0,$* then the expectation in (III.4.20) is no longer required. Letting $\lambda_0 = \lambda\sqrt{E_b N_{0d}}$, then after some simplification, we obtain the following result:

$$D = \begin{cases} 1; \; \hat{u}_n = u_n \\[1em] \min_{\lambda_0}\left\{ \sum_{i=1}^{N_\nu}\sum_{j=1}^{N_\nu} w_i' w_j' \exp\left[\lambda_0^2 - 2\lambda_0\sqrt{\rho_d}\,\frac{\sqrt{\rho_u} + N_i'}{\sqrt{(\sqrt{\rho_u} + N_i')^2 + N_j'^2}}\right]\right\}; \\[1em] \hat{u}_n \neq u_n \end{cases}$$

$$(III.4.24)$$

*In the next part of this section we shall consider an example where $i(t)$ corresponds to intersymbol interference.

32

where

$$\rho_d \triangleq \frac{r^2 T}{2N_{0d}} = \text{downlink signal-to-noise ratio}$$

$$\rho_u \triangleq \frac{E_b}{N_{0u}} = \text{uplink signal-to-noise ratio}$$

(III.4.25)

and we have also replaced $u_n N_i'$ by N_i' since the N_i' values are symmetric around zero. Figure 7 illustrates D versus ρ_d with ρ_u as a parameter using 11-point Gauss-Quadrature, i.e., $N_\nu = 11$.

Another simplification of (III.4.4) assumes that the combined demodulation and detection operations as represented by the integrals in this equation are replaced by ideal coherent demodulation followed by low-pass filtering, sampling at the data rate and a mismatched detector (see Figure 8). Here the low-pass filters are assumed to be ideal in the sense of passing the signal components without distortion while limiting the downlink white Gaussian noise to the signal band-width. The above assumption is tantamount to allowing the true continuous-time system to be approximated by a discrete-time model. Such a model which separates the demodulation process from the detection process also allows taking advantage of the low-pass equivalent representation of signals and systems and its mathematical characterization in many ways resembles the two coordinate description of the system just discussed.

We begin by writing the signal component $z(t)$ of the received downlink signal $y(t)$ of (III.4.3) in the form [see (III.2.13)]

$$z(t) = f(R(t)) \cos [g(R(t)) - \bar{g} + n(t)] \cos (\omega_0 t + \bar{g})$$

$$- f(R(t)) \sin [g(R(t)) - \bar{g} + n(t)] \sin (\omega_0 t + \bar{g})$$

$$= z_c(t) \cos (\omega_0 t + \bar{g}) - z_s(t) \sin (\omega_0 t + \bar{g})$$

(III.4.26)

33
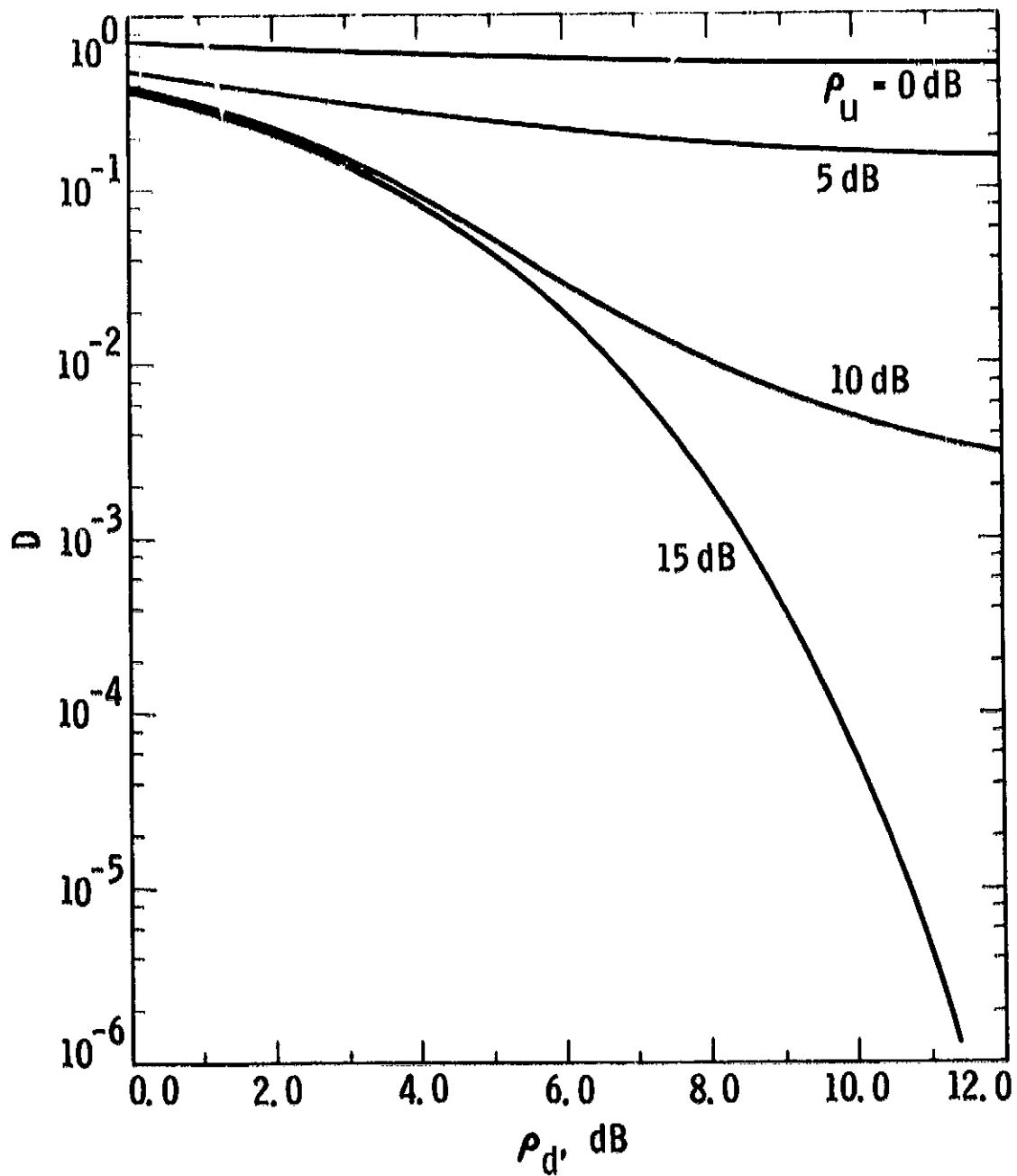
Figure 7. Chernoff Bound D versus Downlink Signal-to-Noise Ratio ρ_d with Uplink Signal-to-Noise Ratio ρ_u as a Parameter

34
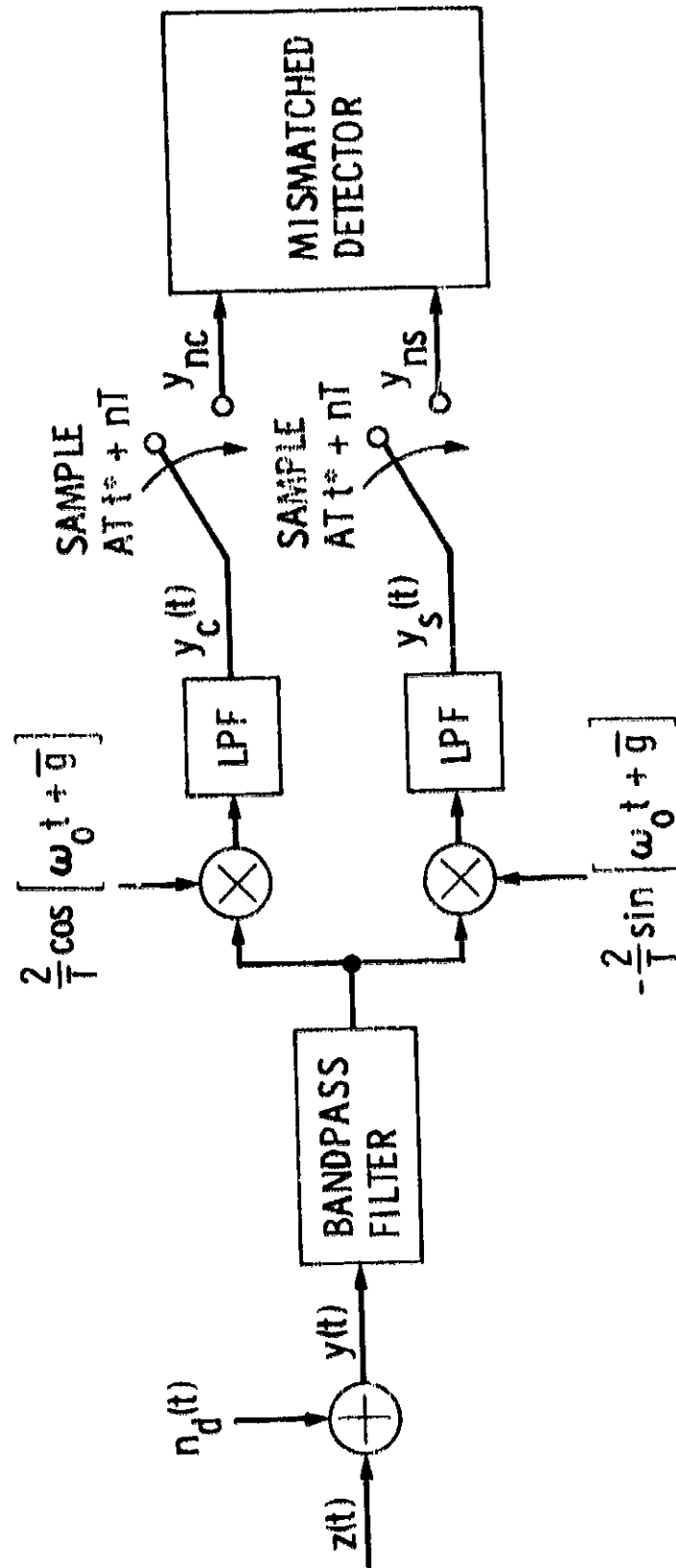
Figure 8. Filter-Sample Receiver

where

$$z_c(t) \triangleq f(R(t)) \cos \left[g(R(t)) - \bar{g} + n(t) \right]$$

(III.4.27a)

and

$$z_s(t) \triangleq f(R(t)) \sin \left[g(R(t)) - \bar{g} + n(t) \right]$$

(III.4.27b)

are slowly varying compared to the carrier oscillations. After quadrature de-modulation by $-2/T \sin (\omega_0 t + \bar{g})$ and $2/T \cos (\omega_0 t + \bar{g})$, the sampled outputs of the ideal low-pass filters at time $t* + nT$ are given by*

$$y_c(t* + nT) = z_c(t* + nT) + n_{dc}(t* + nT)$$

(III.4.28a)

and

$$y_s(t* + nT) = z_s(t* + nT) + n_{ds}(t* + nT)$$

(III.4.28b)

where the downlink noise samples $n_{dc}(t* + nT)$ and $n_{ds}(t* + nT)$ are independent zero mean Gaussian random variables with variance

$$\sigma_d^2 = \frac{N_{0d}}{T}$$

(III.4.29)

Implicit in (III.4.29) is that the noise bandwidth of the ideal low-pass filters is $1/2T$.

_____

*The criterion for selecting $t*$ ($0 \leq t* \leq T$) will be discussed shortly.

The mismatched receiver has the form of the optimum receiver for the uplink signal

$$x(t;s_n,u_n) = x_c(t;s_n,u_n) \cos \omega_0 t$$

$$- x_s(t;s_n,u_n) \sin \omega_0 t \qquad \text{(III.4.30)}$$

transmitted over an ideal additive white Gaussian noise channel. Here $x_c(t;s_n,u_n)$ and $x_s(t;s_n,u_n)$ are the cosine and sine components of the narrowband signal $x(t;s_n,u_n)$ during the $\underline{n\text{th}}$ interval. Defining samples

$$y_{nc} = y_c(t^* + nT),$$

$$y_{ns} = y_s(t^* + nT),$$

$$\hat{x}_{nc} = x_c(t^* + nT; \hat{s}_n,\hat{u}_n),$$

$$\hat{x}_{ns} = x_s(t^* + nT; \hat{s}_n,\hat{u}_n),$$

$$z_{nc} = z_c(t^* + nT),$$

$$z_{ns} = z_s(t^* + nT),$$

$$n_{nc} = n_{dc}(t^* + nT),$$

$$n_{ns} = n_{ds}(t^* + nT), \qquad \text{(III.4.31)}$$

and vectors

$$y_n = \begin{bmatrix} y_{nc} \\ \\ y_{ns} \end{bmatrix}, \qquad \hat{x}_n = \begin{bmatrix} \hat{x}_{nc} \\ \\ \hat{x}_{ns} \end{bmatrix}$$

$$z_n = \begin{bmatrix} z_{nc} \\ \\ z_{ns} \end{bmatrix}, \qquad n_n = \begin{bmatrix} n_{nc} \\ \\ n_{ns} \end{bmatrix}, \qquad (111.4.32)$$

we represent the detector output samples at time $t* + nT$ as

$$y_n = z_n + n_n \qquad (111.4.33)$$

The mismatched receiver uses the metric

$$m(y_n; \hat{s}_n, \hat{u}_n) = (y_n, \hat{x}_n)$$

$$= (z_n, \hat{x}_n) + (n_n, \hat{x}_n) \qquad (111.4.34)$$

which would be optimum if the channel was the ideal linear channel with additive white Gaussian noise.

Using this metric in (111.3.9), we have the Chernoff bound

$$D_\lambda((\hat{s}_n, \hat{u}_n), (s_n, u_n)) = E\left\{\exp\{\lambda[m(y_n; \hat{s}_n, \hat{u}_n) - m(y_n; s_n, u_n)]\}\right\}$$

$$= E\left\{\exp[\lambda(y_n, \hat{x}_n - x_n)]\right\}$$

$$= E\left\{\exp[\lambda(n_n, \hat{x}_n - x_n)]\right\} E\left\{\exp[\lambda(z_n, \hat{x}_n - x_n)]\right\}$$
$$(111.4.35)$$

where the first expectation is over the downlink noise components n_n while the second expectation is over the uplink random variables included in the satellite output signal components z_n. Since

$$E\left\{\exp[\lambda(n_n, \hat{x}_n - x_n)]\right\} = \exp\left\{\frac{1}{2}\lambda^2 \|\hat{x}_n - x_n\|^2 \frac{N_{0d}}{T}\right\} \qquad (111.4.36)$$

we have, analogous to (III.4.8),

$$D_\lambda((\hat{s}_n, \hat{u}_n), (s_n, u_n)) = \exp\left\{ \frac{1}{2} \lambda^2 \| \hat{x}_n - x_n \|^2 \frac{N_0 d}{T} \right\}$$

$$\times E\left\{ \exp[\lambda(z_n, \hat{x}_n - x_n)] \right\} \tag{III.4.37}$$

As noted earlier, this parameter is directly related to the cutoff rate of the channel and is useful in computing transfer function bounds for receivers that use the Viterbi algorithm with the above metric.

4.1.1 Example of MPSK with Intersymbol Interference

Consider the system shown in Figure 9 where the bandlimiting filter at the transmitter determines the channel bandwidth and introduces intersymbol interference. The ideal transmitted M-ary phase modulated signal has the form

$$s(t) = A \sum_{k=-\infty}^{\infty} p(t - kT) \cos[\omega_0 t + \theta_k] \tag{III.4.38}$$

where $\{\theta_k\}$ are i.i.d. random phases taking values in $\{0 = \frac{2\pi}{M} m; \ m = 0, 1, \ldots, M-1\}$ with equal probability. Here $p(t)$ is given by

$$p(t) = \begin{cases} 1; & 0 \le t \le T \\ \\ 0; & \text{otherwise} \end{cases} \tag{III.4.39}$$

We characterize the impulse response of the bandlimiting transmit filter by $h_0(t)$. The filtered transmitted signal has the form

$$x(t) = s(t) * h_0(t)$$

$$= A \sum_{k=-\infty}^{\infty} h(t - kT) \cos[\omega_0 t + \psi(t - kT) + \theta_k] \tag{III.4.40}$$

39
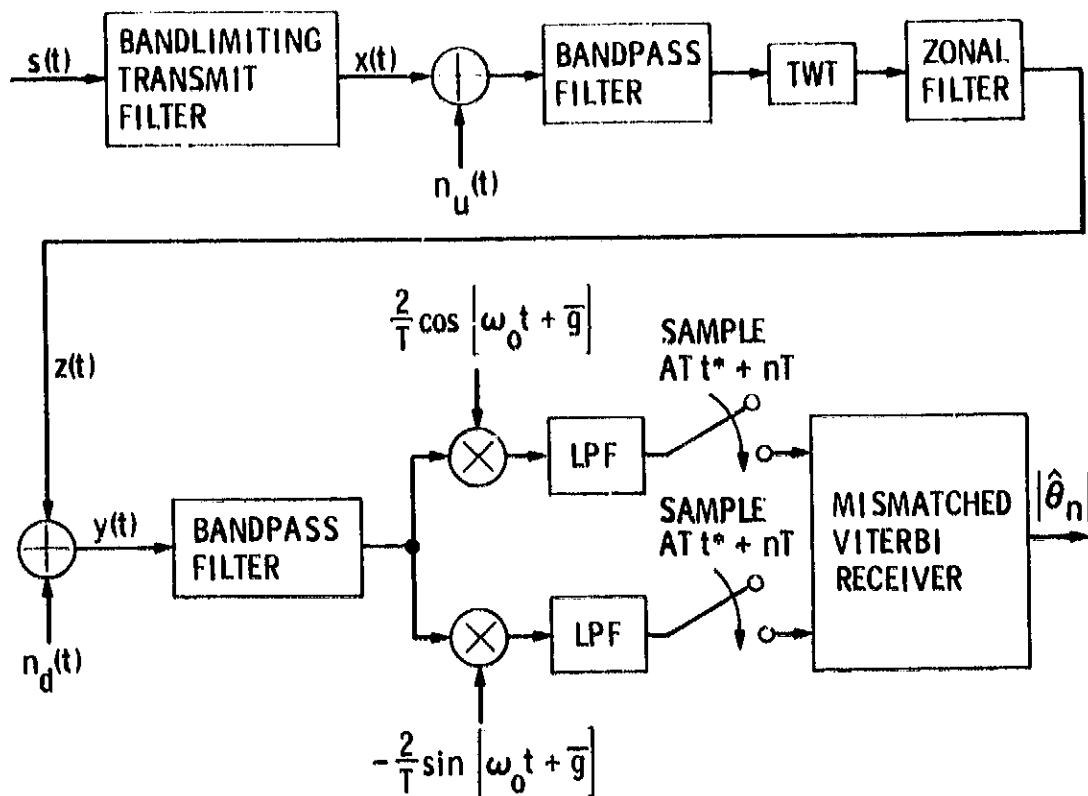
Figure 9. A Satellite ...tem Model for MPSK Modulation with Intersymbol Interference

where $h(t)$ and $\psi(t)$ are the envelope and phase functions of the filtered pulse shape. In general, these two functions spread over an infinite number of signalling intervals. However, in any practical case, we may assume that the intersymbol interference has finite span. Thus, assuming that $h(t)$ and $\psi(t)$ are spread over an LT-second interval, we define $\nu = L-1$ as the memory of the channel. Further defining the translated and T-sec truncated versions of $h(t)$ and $\psi(t)$ by

$$h_i(t) = \begin{cases} h(t + iT); & 0 \le t \le T \\ \\ 0; & \text{otherwise} \end{cases}$$

$$\psi_i(t) = \begin{cases} \psi(t + iT); & 0 \le t \le T \\ \\ 0; & \text{otherwise} \end{cases} \qquad (III.4.41)$$

then the uplink signal in the interval $kT \leq t \leq (k+1)T$ can be written in the form

$$x(t; s_k, u_k) = A \sum_{i=0}^{\nu} h_i(t - kT) \cos [\omega_0 t + \psi_i(t - kT) + \theta_{k-i}]$$

(III.4.42)

where

$$\theta_\ell = \frac{2\pi}{M} u_\ell; \quad u_\ell \in \{0, 1, \ldots, M-1\}$$

(III.4.43)

and

$$s_k = (u_{k-1}, u_{k-2}, \ldots, u_{k-\nu})$$

(III.4.44)

Furthermore, in view of (III.4.30) the low-pass quadrature signal samples are given by

$$x_{kc} = x_c(t^* + kT; s_k, u_k)$$

$$= A \sum_{i=0}^{\nu} h_i(t^*) \cos [\psi_i(t^*) + \theta_{k-i}]$$

(III.4.45a)

and

$$x_{ks} = x_s(t^* + kT; s_k, u_k)$$

$$= A \sum_{i=0}^{\nu} h_i(t^*) \sin [\psi_i(t^*) + \theta_{k-i}]$$

(III.4.45b)

4.1.1.1   Memoryless Receiver

Consider first the simple case of BPSK modulation (M=2), a hard-limited channel [see (III.2.14)], and a memoryless receiver* that uses the decision rule:**

Choose $\hat{\theta}_n = 0$ ($u_n = 0$) if and only if $y_{nc} > 0$

Choose $\hat{\theta}_n = \pi$ ($u_n = 1$) if and only if $y_{nc} \leq 0$

Assuming $\theta_n = 0$ without any loss in generality, then the probability of bit error is

$$P_b = \Pr\left|y_{nc} < 0 \,\middle|\, u_n = 0\right|$$

$$= \Pr\left|z_{nc} + n_{nc} < 0 \,\middle|\, u_n = 0\right|$$

$$= E\left\{Q\left(\frac{z_{nc}}{\sqrt{N_{0d}/T}}\right)\right\} \qquad\qquad (III.4.46)$$

where the expectation is over the intersymbol interference and uplink noise. Here

$$z_{nc} = z_c(t^*+nT)$$

$$= \gamma \cos\left[\eta(t^*+nT)\right]$$

---

*This is the limit of the Viterbi algorithm with the assumed memory $\hat{\nu} = 0$.
**Actually in a real system, y_{nc} would be used to make a decision on θ_{n-i^*} (or equivalently u_{n-i^*}) where i^* depends on the criterion for selecting the "best" sampling point as well as the transmit filter bandwidth-symbol time product. Typically, in analyses of this type [17,21,33-35], it is assumed (and we shall do so) that t^* is chosen to correspond to the peak of the filtered pulse response even though this may not necessarily be the optimum point from the standpoint of minimum bit error probability. Under this assumption, i^* corresponds to the number of symbol times prior to the occurrence of the peak. For simplicity of notation, we shall ignore this inherent delay in making a decision with the understanding that the degradation due to intersymbol interference will always include the appropriate ν pulse response samples both prior to and succeeding the pulse peak despite the fact that we continue to write our summations as going from $i=1$ to $i=\nu$.

$$
= \gamma \frac{x_c(t*+nT) + n_{uc}(t*+nT)}{\sqrt{\left[x_s(t*+nT) + n_{us}(t*+nT)\right]^2 + \left[x_c(t*+nT) + n_{uc}(t*+nT)\right]^2}}
$$

$$
= \gamma \frac{\sum_{i=0}^{\nu} h_i(t*) \cos\left[\psi_i(t*) + \theta_{n-i}\right] + \tilde{n}_{nc}}{\sqrt{\left[\Lambda \sum_{i=0}^{\nu} h_i(t*) \sin\left[\psi_i(t*) + \theta_{n-i}\right] + \tilde{n}_{ns}\right]^2 + \left[\Lambda \sum_{i=0}^{\nu} h_i(t*) \cos\left[\psi_i(t*) + \theta_{n-i}\right] + \tilde{n}_{nc}\right]^2}}
$$

$$
(III.4.47)
$$

where $\tilde{n}_{uc}$ and $\tilde{n}_{us}$ are independent zero mean Gaussian random variables with variance σ_u^2.

Next suppose that we have a 3-pole Butterworth transmit filter whose equivalent low-pass version has the impulse response

$$
\tilde{h}_o(t) = 2\pi B \left[e^{-2\pi Bt} - \frac{2}{\sqrt{3}} e^{-\pi Bt} \cos(\pi\sqrt{3}Bt + \pi/6)\right] u(t)
$$

$$
(III.4.48)
$$

where $u(t)$ is the unit step function and B is the low-pass 3-dB bandwidth of the filter (2B is the RF 3 dB bandwidth assumed symmetric around the carrier frequency ω_0). The response of the equivalent low-pass filter to the rectangular pulse of (III.4.39) is then given by

$$
\tilde{p}(t) = p(t) * \tilde{h}_o(t)
$$

$$
= \begin{cases} r(t) - r(0); & 0 \le t \le T \\ r(t) - r(t-T); & T \le t \le \infty \end{cases}
$$

$$
(III.4.49)
$$

43

where

$$\beta(t) = -\exp(-2\pi B t) - \frac{2}{\sqrt{3}} \exp(-\pi B t) \sin(\pi\sqrt{3} B t)$$

$$(III.4.50)$$

Figure 10 is an illustration of $\overset{\nu}{p}(t)$ versus t/T for various values of BT. Assuming that the ratio of carrier frequency ω_0 to filter bandwidth is large, then the in-phase bandpass pulse response $h(t) \cos \psi(t)$ is approximately equal to the baseband pulse response $\overset{\nu}{p}(t)$ and the quadrature phase pulse response $h(t) \sin \psi(t)$ is approximately equal to zero.

Letting $\overset{\nu}{p}_i(t)$ be defined in terms of $p(t)$ in the manner of (III.4.41) then since $\theta_{n-i} = 0$ or π for all n and $i = 0, 1, \ldots, \nu$, (III.4.47) simplifies to

$$z_{nc} = \gamma \frac{A \sum_{i=0}^{\nu} \cos \theta_{n-i} \, \overset{\nu}{p}_i(t^*) + \overset{\nu}{n}_{nc}}{\sqrt{\overset{\nu}{n}_{ns}^2 + \left[A \sum_{i=0}^{\nu} \cos \theta_{n-i} \, \overset{\nu}{p}_i(t^*) + \overset{\nu}{n}_{nc} \right]^2}}$$

$$(III.4.51)$$

or isolating the intersymbol interference

$$z_{nc} = \gamma \frac{A \, \overset{\nu}{u}_n \, \overset{\nu}{p}(t^*) + A \sum_{i=1}^{\nu} \overset{\nu}{u}_{n-i} \, \overset{\nu}{p}_i(t^*) + \overset{\nu}{n}_{nc}}{\sqrt{\overset{\nu}{n}_{ns}^2 + \left[A \, \overset{\nu}{u}_n \, \overset{\nu}{p}(t^*) + A \sum_{i=1}^{\nu} \overset{\nu}{u}_{n-i} \, \overset{\nu}{p}_i(t^*) + \overset{\nu}{n}_{nc} \right]^2}}$$

$$(III.4.52)$$

where

$$\overset{\nu}{u}_\ell \overset{\Delta}{=} (-1)^{u_\ell}$$
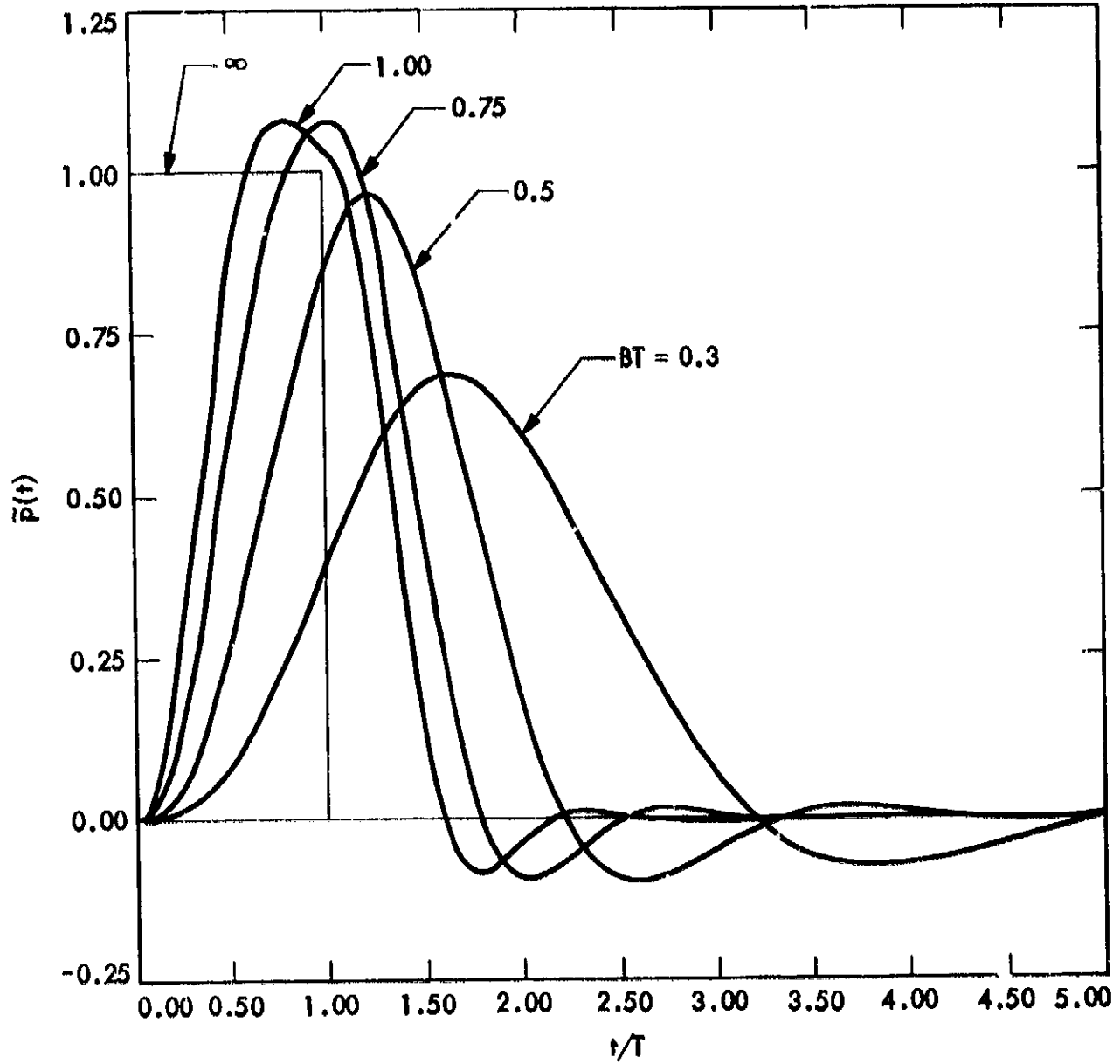
$$(III.4.53)$$

Figure 10. The Response of a Three-Pole Butterworth Filter to a T-sec Rectangular Input Pulse for Various Values of BT

is the ± 1 equivalent representation of the ℓth $(0,1)$ data bit a_ℓ. In (III.4.52), we have also made use of the fact that $\tilde{p}_0(t*) \overset{\Delta}{=} \tilde{p}(t*)$.

To proceed further, we must relate the signal amplitude A to the transmitted uplink average power S. When this is done we can then relate A/σ_u to the uplink signal-to-noise power ratio. Using (III.4.40) for the special case being considered, we define the average transmitted signal power by

$$S = E\left\{\left\langle x^2(t)\right\rangle\right\} = \frac{A^2}{2}\left\langle \sum_{n=-\infty}^{\infty} p^2(t-nT)\right\rangle$$

$$= \frac{A^2}{2T}\int_0^\infty \tilde{p}^2(t)dt$$

$$= \frac{A^2}{2T}\sum_{i=0}^{\nu}\int_0^T \tilde{p}_i^2(t)dt$$

$$\overset{\Delta}{=} \alpha A^2 \tag{III.4.54}$$

where $<\,>$ denotes time average. Thus, the uplink signal-to-noise power ratio ρ_u is given by

$$\rho_u \overset{\Delta}{=} \frac{S}{\sigma_u^2} = \alpha\left(\frac{A}{\sigma_u}\right)^2 \tag{III.4.55}$$

where

$$\alpha \overset{\Delta}{=} \frac{1}{2T}\sum_{i=0}^{\nu}\int_0^T \tilde{p}_i^2(t)dt \tag{III.4.56}$$

For the three-pole Butterworth filter with pulse response of (III.4.49), α is evaluated as[*]

$$\alpha = \frac{1}{2}\left[1 - \frac{1}{6\pi BT}\left\{2 - e^{-2\pi BT} - e^{-\pi BT}\left[\cos\sqrt{3}\pi BT - \sqrt{3}\sin\sqrt{3}\pi BT\right]\right\}\right]$$

(III.4.57)

which varies monotonically as a function of BT from zero (at $BT = 0$) to one-half (at $BT = \infty$).

The evaluation of (III.4.46) using (III.4.52) can be accomplished by applying the moment technique discussed in Reference 1. In this regard, there are two approaches which can be taken and we shall discuss them both along with their relative merits.

The first approach lumps the uplink noise and intersymbol interference together and uses the moments of this combined interference to effect a solution. Specifically, we rewrite (III.4.46) as[**]

$$P_b = E\left\{Q\left(\sqrt{2\rho_d}\,\frac{\tilde{u}_0\sqrt{\frac{\rho_u}{\alpha}}\,\tilde{p}(t^*) + U}{\sqrt{W_s^2 + \tilde{u}_0\left(\sqrt{\frac{\rho_u}{\alpha}}\,\tilde{p}(t^*) + U\right)^2}}\right)\right\}$$

$$= \frac{1}{2}E\left\{Q\left(\sqrt{2\rho_d}\,\frac{\sqrt{\frac{\rho_u}{\alpha}}\,\tilde{p}(t^*) + U}{\sqrt{W_s^2 + \left(\sqrt{\frac{\rho_u}{\alpha}}\,\tilde{p}(t^*) + U\right)^2}}\right)\right\}$$

$$+ \frac{1}{2}E\left\{Q\left(\sqrt{2\rho_d}\,\frac{-\sqrt{\frac{\rho_u}{\alpha}}\,\tilde{p}(t^*) + U}{\sqrt{W_s^2 + \left(-\sqrt{\frac{\rho_u}{\alpha}}\,\tilde{p}(t^*) + U\right)^2}}\right)\right\}$$

$$\triangleq \frac{1}{2}E\left\{P_{b_+}(U, W_s)\right\} + \frac{1}{2}E\left\{P_{b_-}(U, W_s)\right\}$$

(III.4.58)

---

[*]For the purpose of obtaining α as a closed form expression, we have let the memory ν be equal to infinity.

[**]For simplicity of notation, we set $n = 0$.

47

where

$$\mu_d \overset{\Delta}{=} \frac{\gamma^2}{2\sigma_d^2} = 2N_{0d}/T \tag{III.4.59}$$

is the downlink signal-to-noise power ratio,

$$U \overset{\Delta}{=} \sqrt{\frac{\mu_u}{\alpha}} \sum_{i=1}^{\nu} \tilde{u}_{-i} p_i(t^*) + W_c \tag{III.4.60}$$

and W_c, W_s are independent zero mean, unit variance Gaussian random variables. Since U consists of a sum of independent random variables, we can easily (using linear recursion techniques) get the moments of U in terms of the moments of each term in the sum (see Section V of [42]). Furthermore, since W_s is independent of U, we can apply the one-dimensional moment technique twice in a way that is analogous to the two-dimensional Gauss-Quadrature rule used in arriving at (III.4.21). Before formally writing down the solution, however, we must first evaluate the moments of U and W_s.

The random variable U contains a single Gaussian noise random variable W_c whose moments are given by

$$\mu_k^W = E\left\{W_c^k\right\} = \begin{cases} (k-1)!! & ; \ k \text{ even} \\ \\ 0; & k \text{ odd} \end{cases} \tag{III.4.61}$$

Clearly (III.4.61) also characterizes the moments of W_s. However, since W_s is not linearly combined with the intersymbol interference random variables, the expectation over W_s is most easily performed using a Gauss-Hermite quadrature formula analogous to that in (III.4.21).* The remaining terms in U are intersymbol interference from the transmitted pulse response samples.

_____

*Using the moment technique to perform the expectation on W_s would produce identical results to that obtained from the Gauss-Hermite quadrature formula.

48

The moments of these terms are

$$
\mu_k''(1) = E\left\{\left[\sqrt{\tfrac{P_u}{\alpha}\ddot{u}_{-1}\ddot{p}_1(t*)}\right]^k\right\} = \left\{\begin{array}{l}\left[\sqrt{\tfrac{P_u}{\alpha}\ddot{p}_1(t*)}\right]^k ; \ k \ \text{even} \\[2mm] 0; \ k \ \text{odd}\end{array}\right.
$$

(III.4.62)

Using the recursive algorithm discussed in [42; Section V], we can immediately obtain the moments of U, namely,

$$
\mu_k^U \triangleq E\left|U^k\right| ; \ k = 0, 1, 2, \ldots
$$

(III.4.63)

In order to apply the computational technique discussed in [42], we must restrict ourselves to a finite set of moments for U. Thus, we now assume the maximum value of k in (III.4.63) is denoted by N, i.e., we compute only N+1 moments for U. This implies that we need only compute the same number of moments in (III.4.61) and (III.4.62).

Thus, given μ_k^U; $k = 0, 1, 2, \ldots, N$, the technique described in [42] computes the approximating probability frequency function*

$$
q_\ell = \hat{Pr}\left|U = x_\ell\right| ; \ \ell = 1, 2, \ldots, N_{\nu_x}
$$

(III.4.64)

Then, using this distribution in (III.4.58), the average bit error probability is approximately computed as

$$
\begin{aligned}
\hat{P}_b &\approx \frac{1}{2} \hat{E}\left|P_{b_+}(U,W_s)\right| + \frac{1}{2}\hat{E}\left|P_{b_-}(U,W_s)\right| \\
&= \frac{1}{2}\sum_{\nu=1}^{N_{\nu_x}}\sum_{m=1}^{N_{\nu_y}} q_\ell w_m\left[P_{b_+}(x_\ell,y_m) + P_{b_-}(x_\ell,y_m)\right]
\end{aligned}
$$

(III.4.65)

*The hat " ^ " is used to denote the word "approximating."

where $\{y_m\}$ and $\{w_m\}$; $m = 1, 2, \ldots , N_{\nu_y}$ are respectively the probability location points and weights determined from the Gauss-Hermite quadrature formula [43]. The algorithms used to compute N_{ν_x}, the probability location points $\{x_\nu\}$ and the probability masses $\{q_\nu\}$, $\nu = 1, 2, \ldots , N_{\nu_x}$ are adequately described in [42] and are not repeated here.

If the moments of the noise random variables and the moments of the inter-symbol interference, as given by (III.4.61) and (III.4.62) respectively, are grossly different in magnitude, then the algorithms for obtaining the distribution points and probability masses are quite sensitive to the accuracy with which the moments of U are computed. In these situations, it is better to separate the noise from the intersymbol interference and average over each independently. To see how this is done, we first rewrite (III.4.51) as (again assuming n = 0)

$$z_{0c} = \gamma \frac{\sqrt{\frac{\rho_u}{\alpha}} \sum_{i=0}^{\nu} \tilde{u}_{-i} \tilde{p}_i(t^*) + W_c}{\sqrt{W_s^2 + \left[\sqrt{\frac{\rho_u}{\alpha}} \sum_{i=0}^{\nu} \tilde{u}_{-i} \tilde{p}_i(t^*) + W_c\right]^2}}$$

$$= \gamma \frac{V + W_c}{\sqrt{W_s^2 + (V+W_c)^2}}$$

$$= \gamma \cos \eta \qquad\qquad (III.4.66)$$

In (III.4.66), η represents the phase of the output of an envelope detector whose input is signal (V) plus bandpass noise. As such, η has the conditional probability density function

$$p(\eta|V) = \frac{1}{2\pi} \exp (-\rho) + \frac{\sqrt{\rho}\cos \eta}{2\sqrt{\pi}} \exp [-\rho(1 - \cos^2 \eta)]$$

$$\times \text{erfc}[-\sqrt{\rho} \cos \eta]; \quad |\eta| \leq \pi$$

$$\triangleq h(\rho, \cos \eta) \qquad\qquad (III.4.67)$$

where

$$\rho = \frac{V^2}{2} \qquad (III.4.68)$$

with

$$V = \sqrt{\frac{\rho_u}{\alpha}} \sum_{i=0}^{\nu} \tilde{u}_{-i}\tilde{p}_i(t^*)$$

$$= \sqrt{\frac{\rho_u}{\alpha}}\, \tilde{u}_0 \tilde{p}(t^*) + \sqrt{\frac{\rho_u}{\alpha}} \sum_{i=1}^{\nu} \tilde{u}_{-i}\tilde{p}_i(t^*)$$

$$\overset{\triangle}{=} \sqrt{\frac{\rho_u}{\alpha}}\left[\tilde{u}_0 \tilde{p}(t^*) + \mathcal{U}\right] \qquad (III.4.69)$$

Note that from (III.4.60),

$$\mathcal{U} = \sum_{i=1}^{\nu} \tilde{u}_{-i}\tilde{p}_i(t^*) = \left(U - W_c\right)\sqrt{\frac{\alpha}{\rho_u}} \qquad (III.4.70)$$

represents the total intersymbol interference alone. Using (III.4.66) and (III.4.67), it is now a simple matter to compute P_b of (III.4.46), namely,

$$P_b = \frac{1}{2} E\left\{\int_{-\pi}^{\pi} Q\left(\sqrt{2\rho_d}\cos\eta\right) h\left(\rho_+, \cos\eta\right) d\eta\right\}$$

$$+ \frac{1}{2} E\left\{\int_{-\pi}^{\pi} Q\left(\sqrt{2\rho_d}\cos\eta\right) h\left(\rho_-, \cos\eta\right) d\eta\right\} \qquad (III.4.71)$$

51

where the plus and minus on ρ corresponds to V being evaluated with $u_0 = +1$ and -1 respectively and the expectation is now only over the total intersymbol interference $\mathcal{U}$. To evaluate this expectation, we again use the moment technique where the moments of $\mathcal{U}$ are computed by applying the recursive algorithm of [42; Section V] now, however, to only the moments in (III.4.62).

The integrals in (III.4.71) are most easily evaluated using a Gauss-Chebychev quadrature formula [43]. In particular, letting $\theta = \cos \eta$, then

$$\int_{-\pi}^{\pi} Q\left(\sqrt{2\rho_d} \cos \eta\right) h\left(\rho_\pm, \cos \eta\right) d\eta$$

$$= 2 \int_{-1}^{1} Q\left(\sqrt{2\rho_d}\ \theta\right) h\left(\rho_\pm,\ \theta\right) \frac{d\theta}{\sqrt{1 - \theta^2}}$$

$$\cong \frac{2\pi}{N_\nu} \sum_{k=1}^{N_\nu} Q\left(\sqrt{2\rho_d}\ \theta_k\right) h\left(\rho_\pm,\ \theta_k\right) \tag{III.4.72}$$

where

$$\theta_k = \cos \frac{(2k-1)\pi}{2N_\nu}; \quad k = 1, 2, \ldots, N_\nu \tag{III.4.73}$$

and N_ν is chosen depending on the amount of accuracy desired. Finally, then using (III.4.72) in (III.4.71) gives the desired result

$$P_b \cong \frac{\pi}{N_\nu} \hat{E}\left[\sum_{k=1}^{N_\nu} Q\left(\sqrt{2\rho_d}\ \theta_k\right) h\left(\rho_+,\ \theta_k\right) + \sum_{k=1}^{N_\nu} Q\left(\sqrt{2\rho_d}\ \theta_k\right) h\left(\rho_-,\ \theta_k\right)\right] \tag{III.4.74}$$

52

Clearly the disadvantage of (III.4.74) relative to (III.4.65) is the additional computational complexity required to evaluate $h(\rho,\theta)$ for each point in the double summation.

A computer program was written which determines the maximum $\hat{p}_0(t^*)$ of $\hat{p}(t)$ of (III.4.49) (see Figure 10) and the intersymbol interference samples $\hat{p}_i(t^*) = \hat{p}(t^*+iT)$, $i \neq 0$.* The memory v, i.e., the truncation of $\hat{p}(t)$, was chosen such that all $\hat{p}_i(t^*)$ which satisfy $|\hat{p}_i(t^*)|/\hat{p}_0(t^*) < \epsilon$ were set to zero. Typically, it has been determined experimentally that a value of $\epsilon = 10^{-2}$ is sufficiently small to guarantee the needed accuracy in computing bit error rates on the order of 10^{-6}. Using (III.4.65) or (III.4.74) as appropriate, Figure 11 illustrates the behavior of the average bit error probability P_b versus downlink signal-to-noise power ratio ρ_d with uplink signal-to-noise power ratio ρ_u and filter IF 3 dB bandwidth-symbol time product 2BT as parameters. The particular method of solution for the moment technique used in arriving at the approximating probability frequency distributions for the intersymbol interference (and noise) is the Berlekamp-Massey algorithm [44] whose application to problems of this type is discussed in [42]. From Figure 11, we observe that for a fixed uplink signal-to-noise power ratio ρ_u and IF filter bandwidth - bit time product 2BT, there exists an irreducible average bit error probability, say P_{b_∞}, in the limit of infinite downlink signal-to-noise ρ_d. Since

$$\lim_{x \to \infty} Q(x) = \frac{1 - \mathrm{sgn}\, x}{2} \qquad \text{(III.4.75)}$$

then from (III.4.71), this irreducible error probability can be evaluated from the expression

$$P_{b_\infty} = 1 - \frac{1}{2} E \left\{ \int_0^1 [h(\rho_+,\theta) - h(\rho_+,-\theta)] \frac{d\theta}{\sqrt{1 - \theta^2}} \right\}$$

$$- \frac{1}{2} E \left\{ \int_0^1 [h(\rho_-,\theta) - h(\rho_-,-\theta)] \frac{d\theta}{\sqrt{1 - \theta^2}} \right\} \qquad \text{(III.4.76)}$$

*We remind the reader that precursive samples to the pulse peak are included in the intersymbol interference.
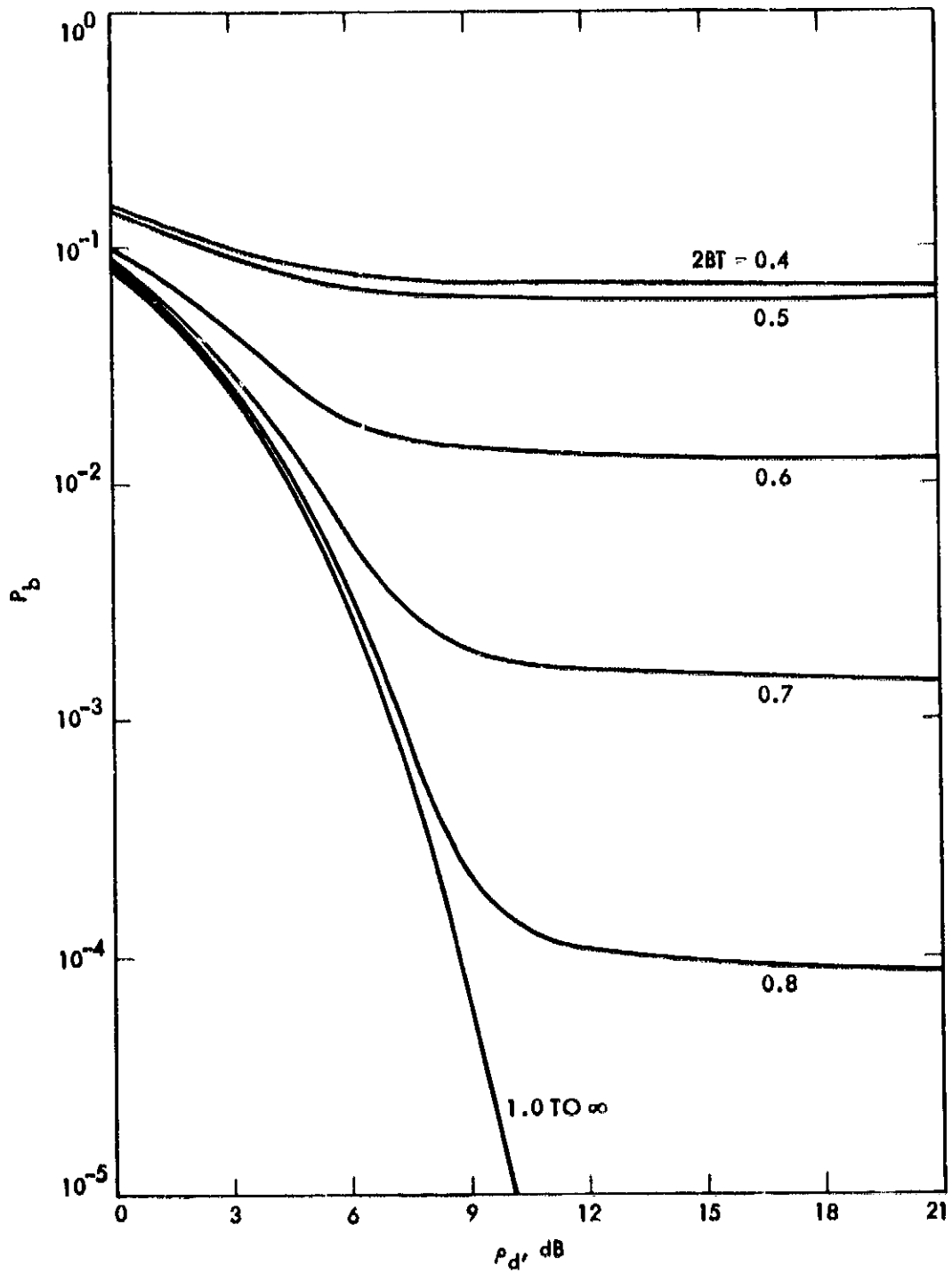
Figure 11a. Average Bit Error Probability of BPSK on a Hard-Limited Satellite Channel versus Downlink Signal-to-Noise Power Ratio with IF Filter Bandwidth – Bit Time Product as a Parameter; Uplink Signal-to-Noise Power Ratio ρ_u = 10 dB.
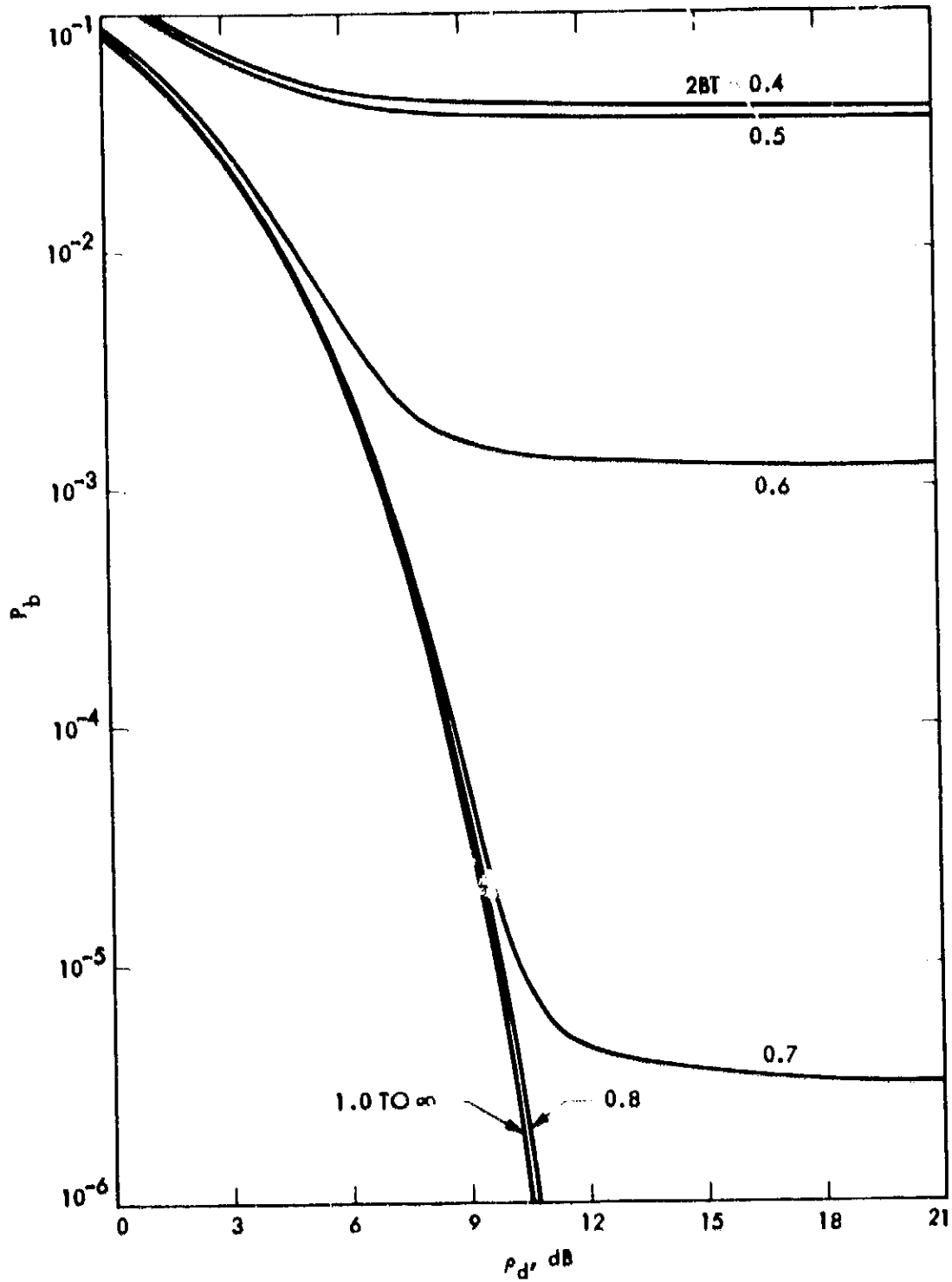
Figure 11b. Average Bit Error Probability of BPSK on a Hard-Limited Satellite Channel versus Downlink Signal-to-Noise Power Ratio with IF Filter Bandwidth - Bit Time Product as a Parameter; Uplink Signal-to-Noise Power Ratio ρ_u = 15 dB.

or using (III.4.67),

$$
P_{b_m} = 1 - \frac{1}{2} E \left\{ \int_0^1 \sqrt{\frac{\rho_+}{\pi}} \, \theta \, \exp\left[-\rho_+(1-\theta^2)\right] \frac{d\theta}{\sqrt{1-\theta^2}} \right\}
$$

$$
- \frac{1}{2} E \left\{ \int_0^1 \sqrt{\frac{\rho_-}{\pi}} \, \theta \, \exp\left[-\rho_-(1-\theta^2)\right] \frac{d\theta}{\sqrt{1-\theta^2}} \right\}
$$

$$
= 1 - \frac{1}{2} E \left\{ \sqrt{\rho_+} \ \text{erf} \ (\sqrt{\rho_+}) \right\} - \frac{1}{2} E \left\{ \sqrt{\rho_-} \ \text{erf} \ (\sqrt{\rho_-}) \right\}
$$

$$(III.4.77)$$

As another example, consider the class of staggered quadrature modulations which includes such well known techniques as staggered QPSK (SQPSK), staggered quadrature overlapped raised cosine (SQORC) [45-47] and minimum-shift-keying (MSK) [48,49]. In particular, the transmitter takes the form illustrated in Figure 12.

Prior to transmitter filtering, a quadrature modulation signal can be expressed as

$$
s(t) = A \left(\sum_{n=-\infty}^{\infty} a_n p(t-2nT) \right) \cos \omega_0 t
$$

$$
+ A \left(\sum_{n=-\infty}^{\infty} b_n p(t-(2n+1)T) \right) \sin \omega_0 t
$$

$$(III.4.78)$$

where as before A is the signal amplitude, ω_0 is the radian carrier frequency, a_n, $b_n = \pm 1$ are the quadrature binary data symbol sequences each transmitted at a rate $1/2T$ symbols/sec (T is the equivalent bit time), and $p(t)$ is the pulse shape. For SQORC modulation, $p(t)$ is given by
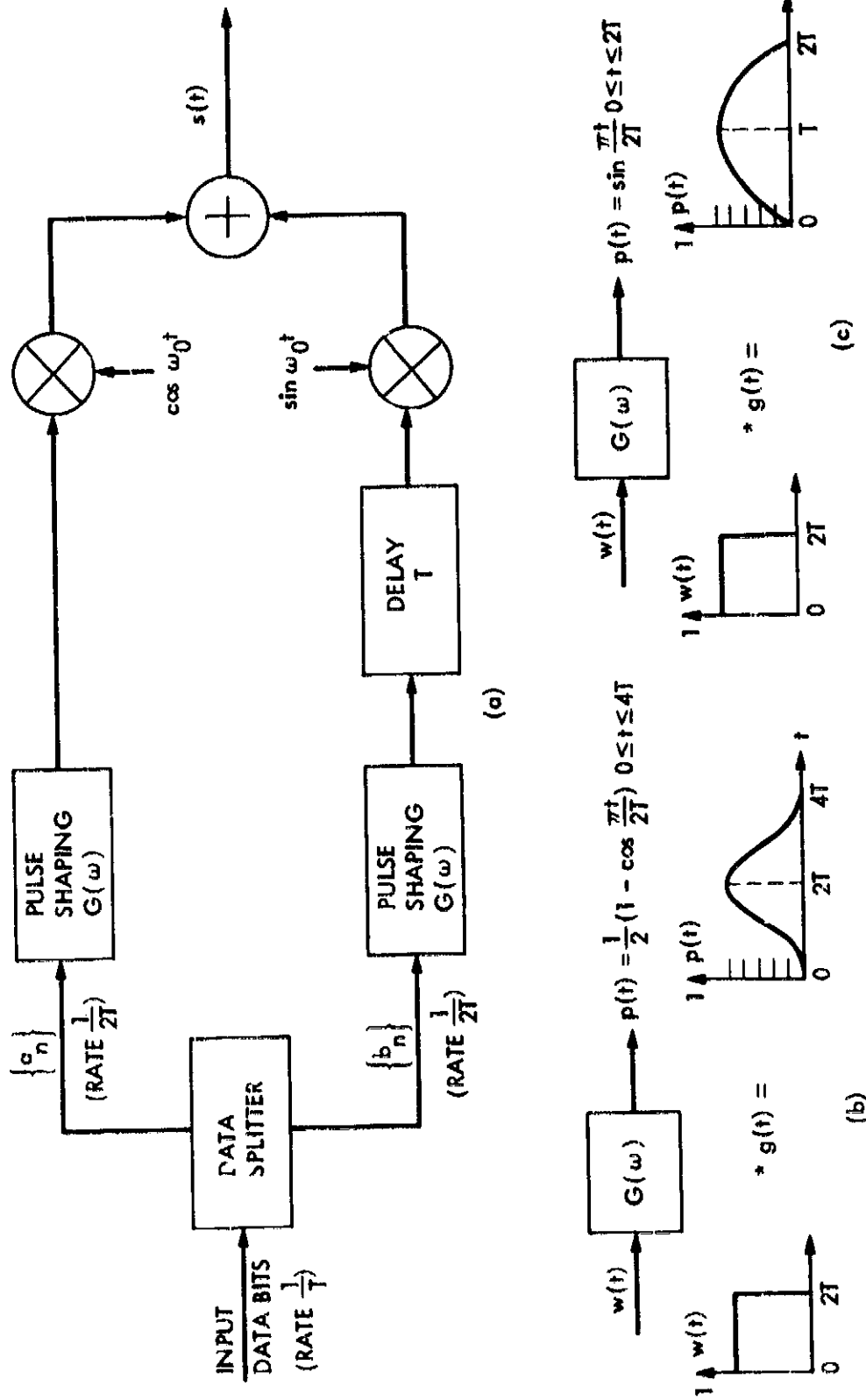
Figure 12. (a) A Staggered Quadrature Modulator. (b) Generation of a Raised-Cosine Pulse for SQORC Modulation. (c) Generation of a Half-Sine Pulse for MSK Modulation.

$$p(t) = \begin{cases} \frac{1}{2}\left(1 - \cos\frac{\pi t}{2T}\right) = \sin^2\frac{\pi t}{4T}; & 0 \le t \le 4T \\ \\ 0; & \text{otherwise} \end{cases} \qquad (\text{III.4.79a})$$

Since the duration of $p(t)$ (i.e., $4T$) is greater than the symbol time $2T$, then clearly the pulses overlap in each data stream; hence, the name SQORC. For MSK modulation, $p(t)$ is given by

$$p(t) = \begin{cases} \sin\frac{\pi t}{2T}; & 0 \le t \le 2T \\ \\ 0; & \text{otherwise} \end{cases} \qquad (\text{III.4.79b})$$

After passing through the transmit filter with impulse responses $h_0(t)$ the signal $s(t)$ of (III.4.78) becomes

$$x(t) = A\left(\sum_{n=-\infty}^{\infty} a_n \tilde{p}(t-2nT)\right) \cos \omega_0 t$$

$$+ A\left(\sum_{n=-\infty}^{\infty} b_n \tilde{p}(t-(2n+1)T)\right) \sin \omega_0 t$$

$$(\text{III.4.80})$$

where $p(t)$ again satisfies the convolution of (III.4.49). Following an approach analogous to that leading to (III.4.58) for the BPSK case, one can show that for staggered quadrature modulations the equivalent relation is given by [47]

$$P_b = E\left\{ Q\left(\sqrt{2\rho_d} \; \frac{u_0\sqrt{\frac{\rho_u}{\alpha}}\,\tilde{p}(t*) + U}{\sqrt{W^2 + \left(u_0\sqrt{\frac{\rho_u}{\alpha}}\,\tilde{p}(t*) + U\right)^2}} \right) \right\}$$

$$- \frac{1}{2} E \left\{ Q \left(\sqrt{2\rho_d} - \frac{\sqrt{\frac{\rho_u}{\alpha}} \hat{p}(t*) + U}{\sqrt{W^2 + \left(\sqrt{\frac{\rho_u}{\alpha}} \hat{p}(t*) + U \right)^2}} \right) \right\}$$

$$+ \frac{1}{2} E \left\{ Q \left(\sqrt{2\rho_d} - \frac{- \sqrt{\frac{\rho_u}{\alpha}} \hat{p}(t*) + U}{\sqrt{W^2 + \left(\sqrt{\frac{\rho_u}{\alpha}} \hat{p}(t*) + U \right)^2}} \right) \right\}$$

$$\triangleq \frac{1}{2} E \left\{ P_{b_+}(U,W) \right\} + \frac{1}{2} E \left\{ P_{b_-}(U,W) \right\} \tag{III.4.81}$$

where U is defined analogous to (III.4.60), namely,

$$U = \sqrt{\frac{\rho_u}{\alpha}} \sum_{i=1}^{\nu} a_{-i} \hat{p}_{2i}(t*) + W_c \tag{III.4.82}$$

and

$$W = \sqrt{\frac{\rho_u}{\alpha}} \sum_{i=1}^{\nu} b_{-i} \hat{p}_{2i-1}(t*) + W_s \tag{III.4.83}$$

Note that now both the inphase and quadrature sampled interferences U and W each contain a single Gaussian noise sample and a sum of intersymbol interference random variables. As before, however, U and W are still independent since the two sets of intersymbol interference terms are independent because of the independence assumption on the quadrature data sequences $\{a_n\}$ and $\{b_n\}$. Thus, one can still

59

apply the one-dimensional moment technique twice to evaluate P_b of (III.4.81) where the statistical average over W now represents a generalization of the simple Gauss-Hermite average previously performed on W_s alone. In particular, two approaches are again possible depending upon whether the noise samples are lumped with the intersymbol interference samples in determining the moments, or the average is performed on the noise and intersymbol interference separately.

In the case of the former, an approximating probability frequency function is found given the moments of W, i.e.,

$$w_\ell = \hat{P}r\left|W{=}y_\ell\right|; \quad \ell = 1, 2, \ldots, N_{\nu_y} \qquad (III.4.84)$$

which together with the previously found approximating frequency function for the moments of U [see (III.4.64)] enables evaluation of (III.4.81) in a manner analogous to (III.4.65).

In the case of the latter, we define [analogous to (III.4.70)]

$$\mathscr{U} = \sum_{i=1}^{\nu} a_{-i}\tilde{P}_{2i}(t^*) = (U - W_c) \sqrt{\frac{\alpha}{\rho_u}} \qquad (III.4.85a)$$

and

$$\mathscr{W} = \sum_{i=1}^{\nu} b_{-i}\tilde{P}_{2i-1}(t^*) = (W - W_s) \sqrt{\frac{\alpha}{\rho_u}} \qquad (III.4.85b)$$

which represent the intersymbol interference alone. Then, analogous to (III.4.71), we now obtain the expression

$$P_b = \frac{1}{2} E\left\{\int_{-\pi}^{\pi} Q\left(\sqrt{2\rho}_d \cos\left[\tan^{-1}\frac{\mathscr{W}}{\tilde{p}(t^*)+\mathscr{U}} + \eta\right]\right)h(\rho_+, \cos \eta)d\eta\right\}$$

$$+ \frac{1}{2} E\left\{\int_{-\pi}^{\pi} Q\left(-\sqrt{2\rho}_d \cos\left[\tan^{-1}\frac{\mathscr{W}}{-\tilde{p}(t^*)+\mathscr{U}} + \eta\right]\right)h(\rho_-, \cos \eta)d\eta\right\}$$

$$(III.4.86)$$

where now

$$\rho_{\pm} = \frac{\rho_u}{2\alpha}\left[(\pm \tilde{p}(t^*)+\mathscr{U})^2 + \mathscr{U}^2\right]$$

(III.4.87)

Again letting $\theta = \cos \eta$ and using a Gauss-Chebychev quadrature formula to evaluate (III.4.86), we get the final result

$$
\begin{aligned}
P_b = \frac{\pi}{2N_\nu}\,\hat{E}\Bigg\{ &\sum_{k=1}^{N_\nu}\Bigg[Q\left(\sqrt{2\rho_d}\ \frac{\theta_k[\tilde{p}(t^*)+\mathscr{U}]-\sqrt{1-\theta_k^{\,2}}\,\mathscr{U}}{\sqrt{\mathscr{U}^2+(\tilde{p}(t^*)+\mathscr{U})^2}}\right) \\
&+ Q\left(\sqrt{2\rho_d}\ \frac{\theta_k[\tilde{p}(t^*)+\mathscr{U}]+\sqrt{1-\theta_k^{\,2}}\,\mathscr{U}}{\sqrt{\mathscr{U}^2+(\tilde{p}(t^*)+\mathscr{U})^2}}\right)\Bigg]\,h(\rho_+,\theta_k) \\
&+\sum_{k=1}^{N_\nu}\Bigg[Q\left(\sqrt{2\rho_d}\ \frac{\theta_k[\tilde{p}(t^*)-\mathscr{U}]-\sqrt{1-\theta_k^{\,2}}\,\mathscr{U}}{\sqrt{\mathscr{U}^2+(\tilde{p}(t^*)-\mathscr{U})^2}}\right) \\
&+ Q\left(\sqrt{2\rho_d}\ \frac{\theta_k[\tilde{p}(t^*)-\mathscr{U}]+\sqrt{1-\theta_k^{\,2}}\,\mathscr{U}}{\sqrt{\mathscr{U}^2+(\tilde{p}(t^*)-\mathscr{U})^2}}\right)\Bigg]\,h(\rho_-,\theta_k)\Bigg\}
\end{aligned}
$$

(III.4.88)

where θ_k is defined in (III.4.73).

To numerically illustrate the above analytical results, we again postulate a 3-pole Butterworth transmit filter as described by the equivalent low-pass impulse response in (III.4.48). Substituting (III.4.48) together with (III.4.76a) or (III.4.76b) into (III.4.49) then allows computation of the pulse response $\tilde{p}(t)$ for either SQORC or MSK modulations. In particular, for the raised cosine pulse shape

$$
\tilde{p}(t) = \begin{cases} \beta(t;t) - \beta(0;t); & 0 \le t \le 4T \\[2em] \beta(t;t) - \beta(t-4T;t); & 4T \le t \le \infty \end{cases}
$$

$$(III.4.89a)$$

where

$$
\beta(\tau;t) = -\frac{1}{2} e^{-2\pi B\tau} - \frac{1}{\sqrt{3}} e^{-\pi B\tau} \sin(\pi\sqrt{3}B\tau)
$$

$$
+ \frac{1}{2} \frac{e^{-2\pi B\tau}}{\sqrt{1 + \left(\frac{1}{4BT}\right)^2}} \cos\left[\frac{\pi B(\tau-t)}{2BT} + \tan^{-1}\left(\frac{1}{4BT}\right)\right]
$$

$$
- \frac{1}{\sqrt{3}} \frac{e^{-\pi B\tau}}{\sqrt{1 + \left(\sqrt{3} - \frac{1}{2BT}\right)^2}} \cos\left[\pi\sqrt{3}B\tau + \frac{\pi}{6} + \frac{\pi B(t-\tau)}{2BT} + \tan^{-1}\left(\sqrt{3} - \frac{1}{2BT}\right)\right]
$$

$$
- \frac{1}{\sqrt{3}} \frac{e^{-\pi B\tau}}{\sqrt{1 + \left(\sqrt{3} + \frac{1}{2BT}\right)^2}} \cos\left[\pi\sqrt{3}B\tau + \frac{\pi}{6} - \frac{\pi B(t-\tau)}{2BT} + \tan^{-1}\left(\sqrt{3} + \frac{1}{2BT}\right)\right]
$$

$$(III.4.89b)$$

While for the MSK pulse,

$$
\tilde{p}(t) = \begin{cases} \beta(t;t) - \beta(0;t); & 0 \le t \le 2T \\[2em] \beta(t;t) - \beta(t-2T;t); & 2T \le t \le \infty \end{cases}
$$

$$(III.4.90a)$$

62

with

$$\beta(\tau;t) = \sqrt{\frac{e^{-2\pi B\tau}}{1 + \left(\frac{1}{4BT}\right)^2}} \sin\left[\frac{\pi B(\tau-t)}{2BT} + \tan^{-1}\left(\frac{1}{4BT}\right)\right]$$

$$+ \frac{2}{\sqrt{3}} \sqrt{\frac{e^{-\pi B\tau}}{1 + \left(\sqrt{3} - \frac{1}{2BT}\right)^2}} \sin\left[\pi\sqrt{3}B\tau + \frac{\pi}{6} + \frac{\pi B(t-\tau)}{2BT} + \tan^{-1}\left(\sqrt{3} - \frac{1}{2BT}\right)\right]$$

$$- \frac{2}{\sqrt{3}} \sqrt{\frac{e^{-\pi B\tau}}{1 + \left(\sqrt{3} + \frac{1}{2BT}\right)^2}} \sin\left[\pi\sqrt{3}B\tau + \frac{\pi}{6} - \frac{\pi B(t-\tau)}{2BT} + \tan^{-1}\left(\sqrt{3} + \frac{1}{2BT}\right)\right]$$

$$(III.4.90b)$$

Figure 13 is an illustration of $\hat{p}(t)$ of (III.4.90a) versus t/T for various values of 2BT. Figures 14 and 15 illustrate the behavior of the average bit error probability P_b versus downlink signal-to-noise power ratio ρ_d with uplink signal-to-noise power ratio ρ_u and filter IF 3-dB bandwidth-symbol time product 2BT as parameters. Again the Berlekamp-Massey algorithm [44] was used to solve the moment problem. Analogous to the results for BPSK, there again exists an irreducible bit error probability P_{b_∞} in the limit of infinite downlink signal-to-noise ratio due to the uplink noise and intersymbol interference. Here this irreducible error probability can be evaluated from the expression

$$P_{b_\infty} = 1 - \frac{1}{2} E\left\{\int_{\theta_+}^1 h(\rho_+,\theta)\frac{d\theta}{\sqrt{1-\theta^2}} - \int_{-\theta_+}^1 h(\rho_+,-\theta)\frac{d\theta}{\sqrt{1-\theta^2}}\right\}$$

$$- \frac{1}{2} E\left\{\int_{\theta_-}^1 h(\rho_-,\theta)\frac{d\theta}{\sqrt{1-\theta^2}} - \int_{-\theta_-}^1 h(\rho_-,-\theta)\frac{d\theta}{\sqrt{1-\theta^2}}\right\}$$

$$(III.4.91)$$

63
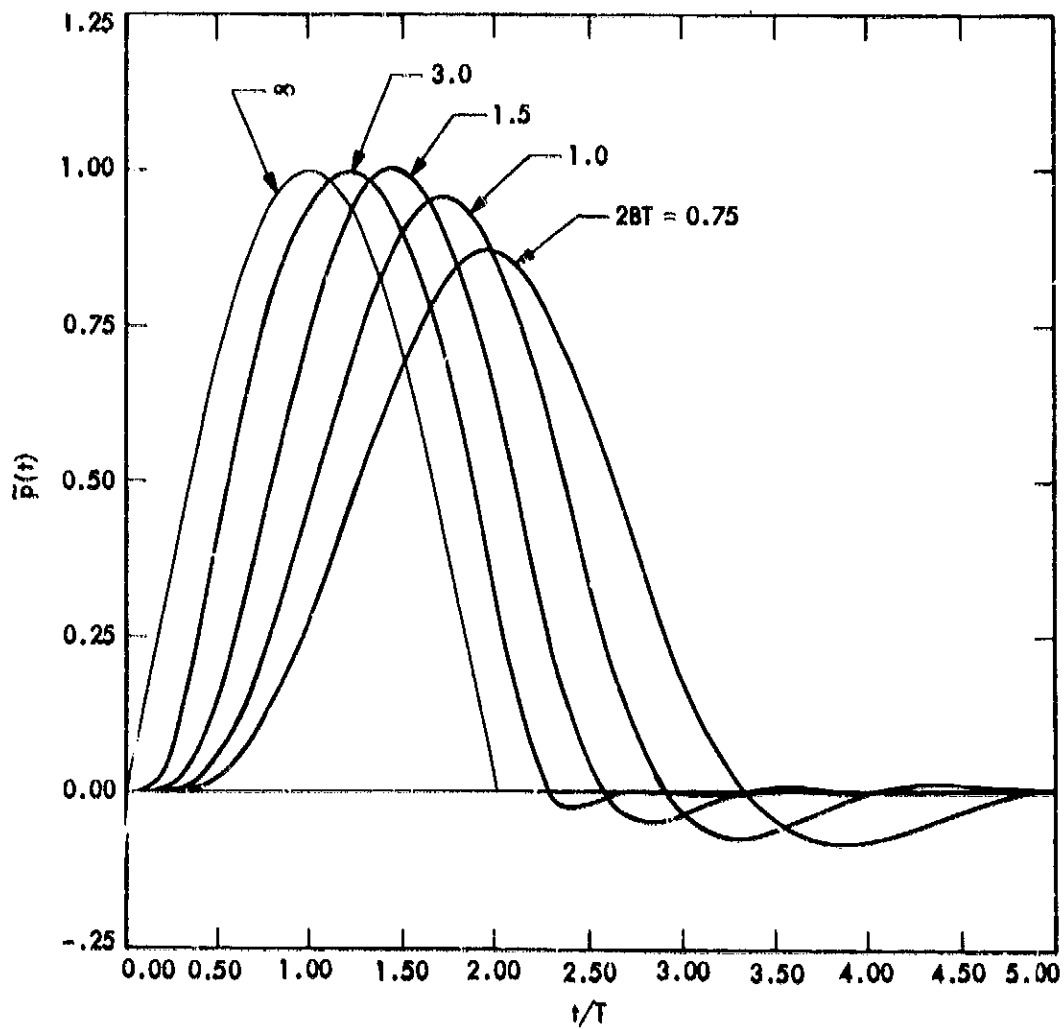
Figure 13. The Response of a Three-Pole Butterworth Filter to a 2T-sec Half-Sinusoid Input Pulse for Various Values of 2BT
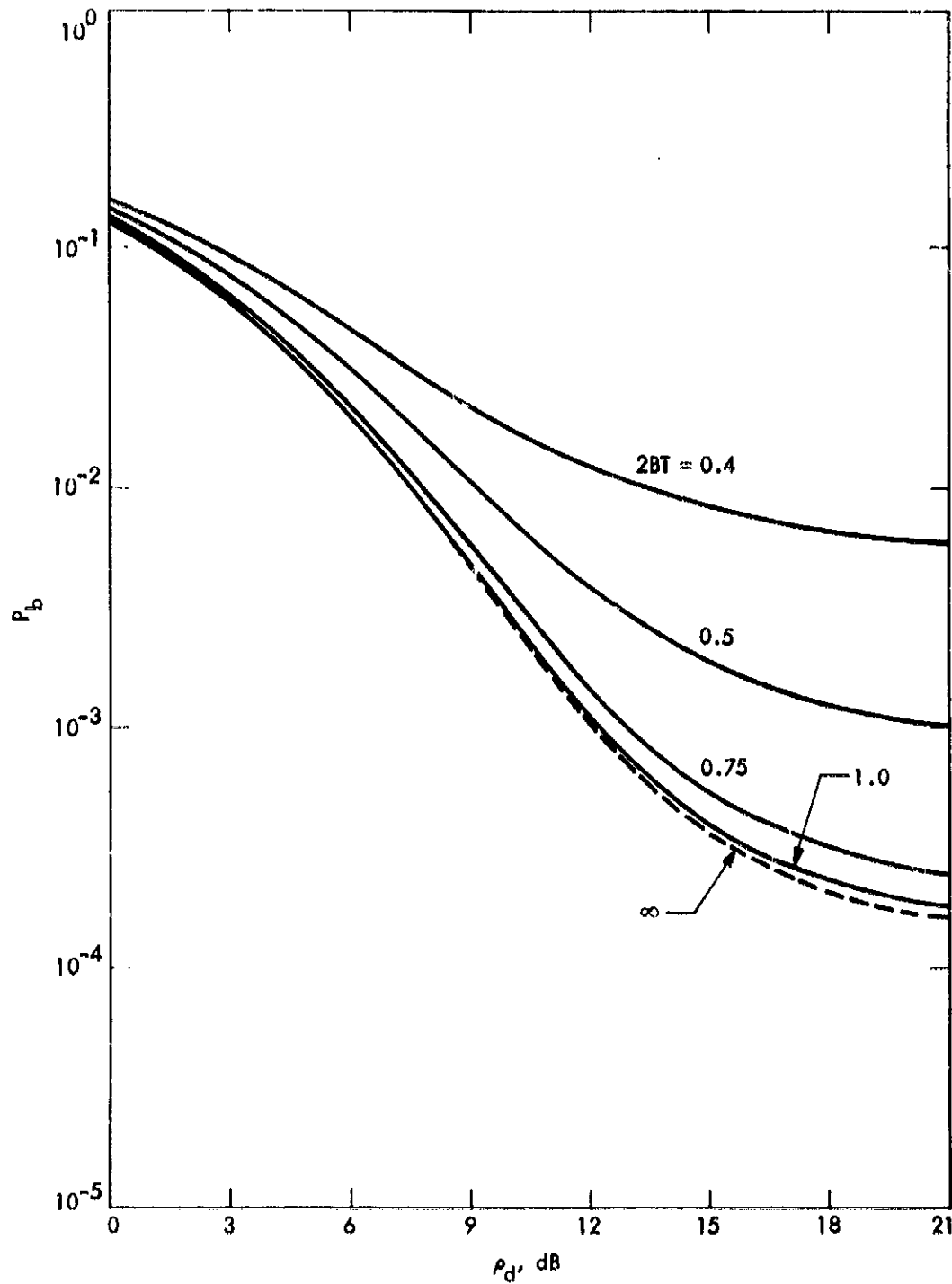
Figure 14a.   Average Bit Error Probability of SQORC on a Hard-Limited Satellite Channel versus Downlink Signal-to-Noise Power Ratio with IF Filter Bandwidth - Bit Time Product as a Parameter; Uplink Signal-to-Noise Power Ratio ρ_u - 10 dB
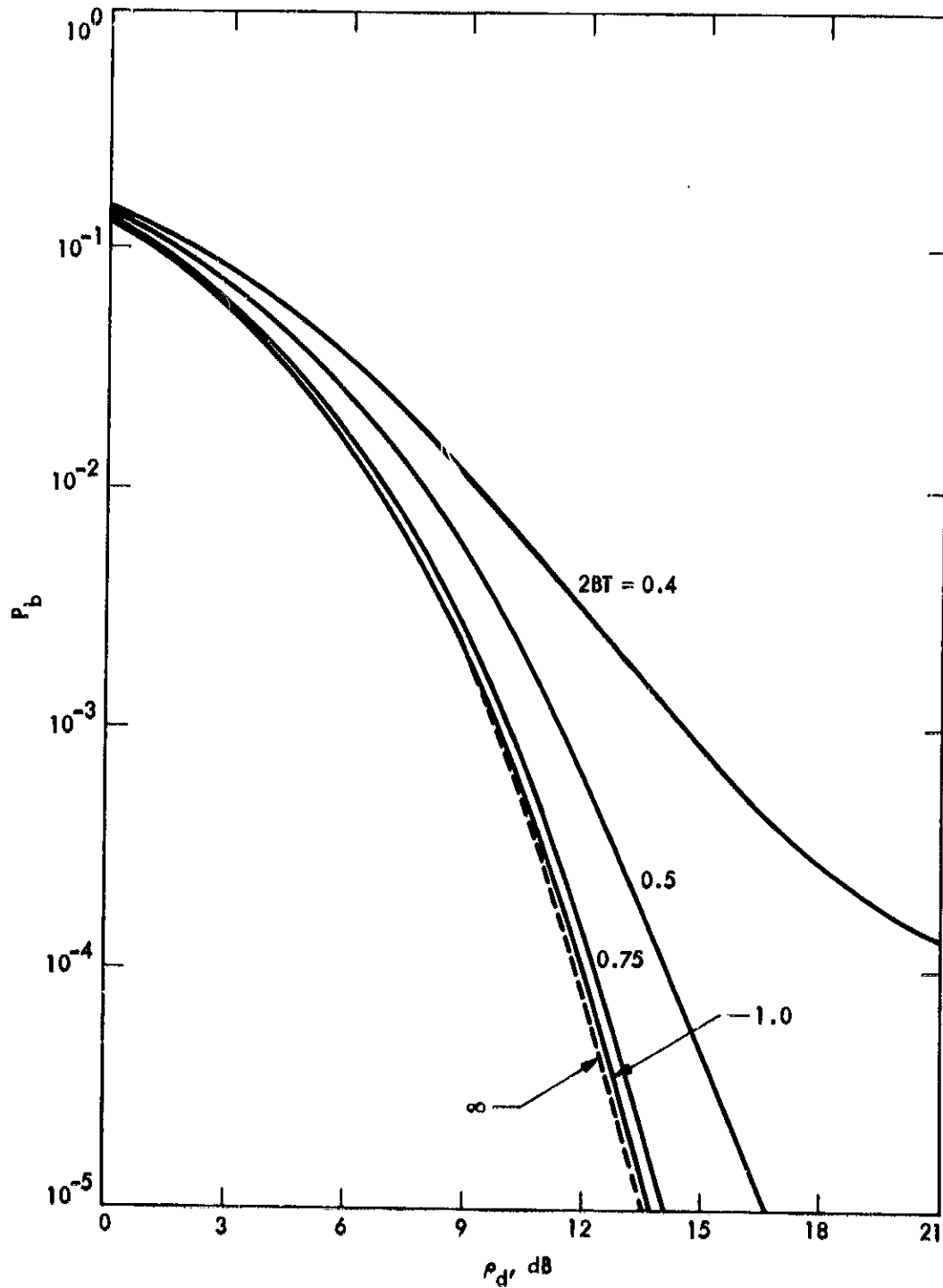
Figure 14b. Average Bit Error Probability of SQORC on a Hard-Limited Satellite Channel versus Downlink Signal-to-Noise Power Ratio with IF Filter Bandwidth - Bit Time Product as a Parameter; Uplink Signal-to-Noise Power Ratio $\rho_u = 15$ dB
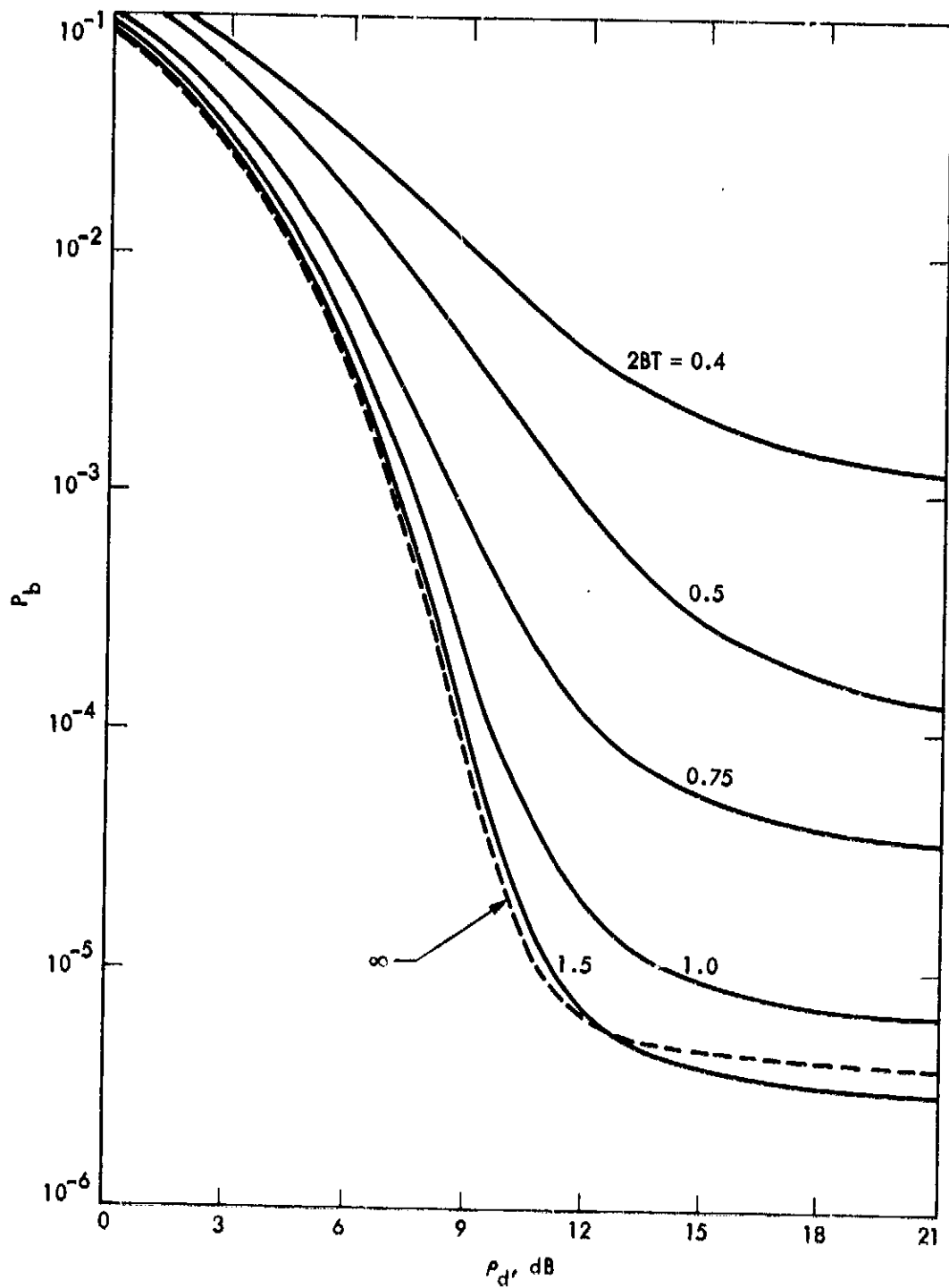
Figure 15a. Average Bit Error Probability of MSK on a Hard-Limited Satellite Channel versus Downlink Signal-to-Noise Power Ratio with IF Filter Bandwidth - Bit Time Product as a Parameter; Uplink Signal-to-Noise Power Ratio ρ_u = 10 dB
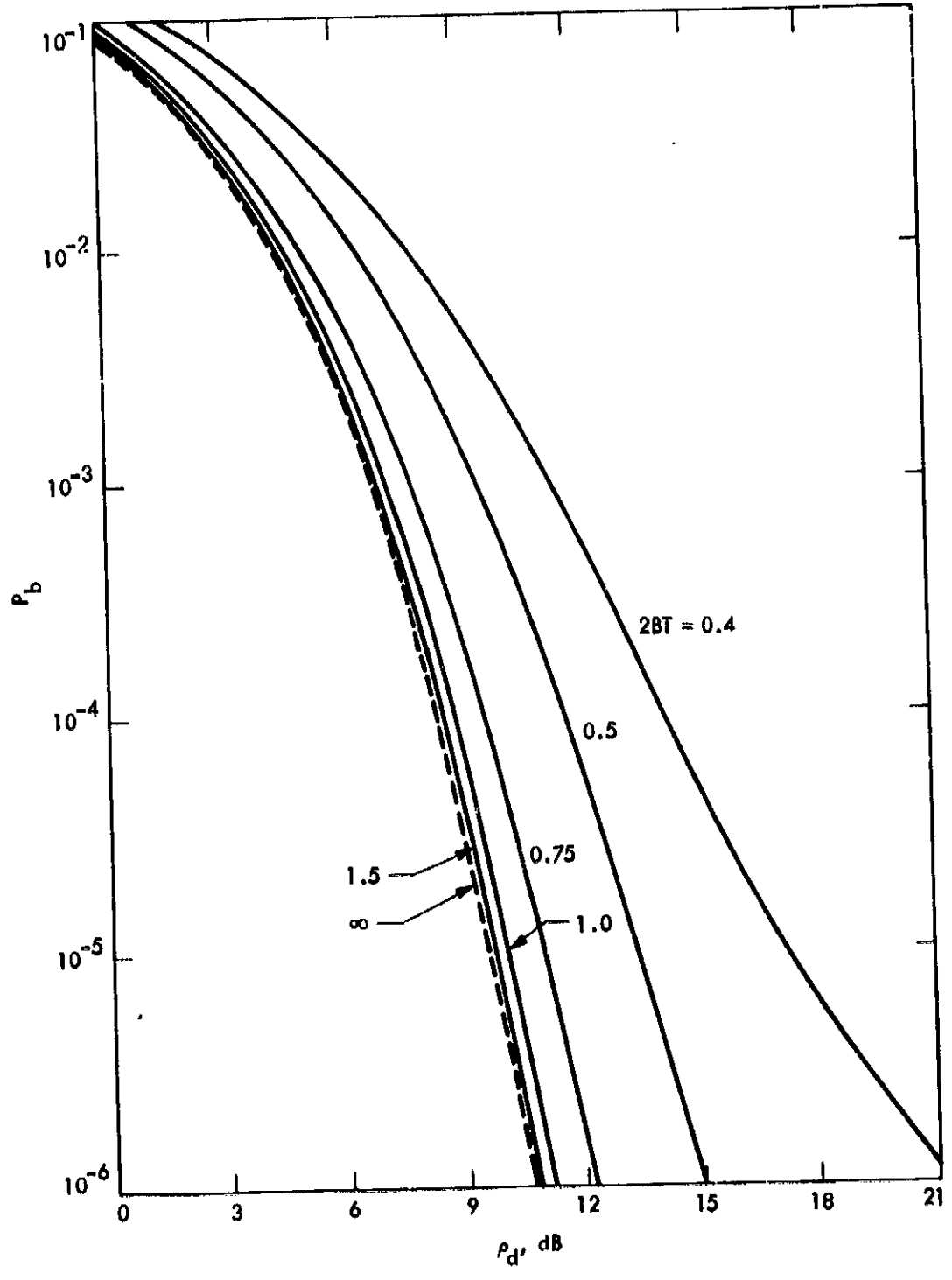
Figure 15b. Average Bit Error Probability of MSK on a Hard-Limited Satellite Channel versus Downlink Signal-to-Noise Power Ratio with IF Filter Bandwidth – Bit Time Product as a Parameter; Uplink Signal-to-Noise Power Ratio ρ_u = 15 dB

where

$$\theta_i \triangleq \frac{\mathcal{H}}{\sqrt{\mathcal{H}^2 + (\dot{p}(t*) + \mathcal{H})^2}} \qquad (\text{III.4.92})$$

Unfortunately, (III.4.91) cannot be obtained in closed form in the same manner that (III.4.76) became (III.4.77).

4.1.1.2   Viterbi Receiver (Maximum-Likelihood Sequence Estimator)

Next let us examine the performance of the mismatched receiver that takes samples y_n computes metrics $m(y_n;s_n,u_n)$ and applies the Viterbi algorithm to the collection of these metrics. Here we assume that the receiver is the maximum-likelihood receiver for the linear intersymbol interference channel with additive white Gaussian noise. The resulting Viterbi algorithm is thus mismatched only in that it ignores uplink noise and the satellite nonlinearities. As already noted many times, the key to evaluating the performance of receivers of this type is the evaluation of the pair-wise error probability of (III.3.8) where now $D_\lambda((\dot{s}_n,\dot{u}_n),(s_n,u_n))$ is given by (III.4.37) which in turn requires evaluation of

$$E\left\{e^{\lambda(z_n,\dot{x}_n - x_n)}\right\}$$

with the expectation being performed over the uplink noise components. The vectors $\dot{z}_n$ and x_n are defined in (III.4.32) and their components in (III.4.31). To emphasize the dependence of these components on the uplink noise samples

$$n_{nc} \triangleq n_{nc}(t* + nT)$$

$$n_{ns} \triangleq n_{ns}(t* + nT) \qquad (\text{III.4.93})$$

which are i.i.d. zero mean Gaussian random variables with variance σ_u^2, and the signal state s_n and data symbol u_n, we rewrite them as

69

$$z_{nc} = z_c(t^*+nT)$$

$$\overset{\Lambda}{=} z_c(s_n, u_n; \hat{n}_{nc}, \hat{n}_{ns})$$

$$= f(R(t^*+nT)) \cos [g(R(t^*+nT)) - \bar{g} + \eta(t^*+nT)]$$

$$z_{ns} = z_s(t^*+nT)$$

$$\overset{\Lambda}{=} z_s(s_n, u_n; \hat{n}_{nc}, \hat{n}_{ns})$$

$$= f(R(t^*+nT)) \sin [g(R(t^*+nT)) - \bar{g} + \eta(t^*+nT)] \qquad (III.4.94a)$$

and

$$\hat{x}_{nc} = x_c(t^*+nT; \hat{s}_n, \hat{u}_n)$$

$$\overset{\Lambda}{=} x_c(\hat{s}_n, \hat{u}_n)$$

$$\hat{x}_{ns} = x_s(t^*+nT; \hat{s}_n, \hat{u}_n)$$

$$\overset{\Lambda}{=} x_s(\hat{s}_n, \hat{u}_n) \qquad (III.4.94b)$$

Finally, then using a Gauss-Hermite quadrature formula to approximate the expectation of the uplink noise components in (III.4.93), $D_\lambda((\hat{s}_n, \hat{u}_n), (s_n, u_n))$ given by (III.4.37) assumes the general form

$$D_\lambda((\hat{s}_n, \hat{u}_n), (s_n, u_n)) = \exp \left\{ \frac{1}{2} \lambda^2 [\left(x_c(\hat{s}_n, \hat{u}_n) - x_c(s_n, u_n) \right)^2 \right.$$

$$+ \left(x_s(\hat{s}_n, \hat{u}_n) - x_s(s_n, u_n) \right)^2] \frac{N_{0d}}{T}$$

$$\cdot \sum_{i=1}^{N_v} \sum_{j=1}^{N_v} w_i w_j \exp \left\{ \lambda \left[z_c(s_n, u_n; N_i, N_j) \left(x_c(\hat{s}_n, \hat{u}_n) - x_c(s_n, u_n) \right) \right. \right.$$

$$\left. \left. + z_s(s_n, u_n; N_i, N_j)(x_s(\hat{s}_n, \hat{u}_n) - x_s(s_n, u_n)) \right] \right\} \right\}$$

$$(III.4.95)$$

70

where analogous to (III.4.21), $\{N_1\}$ are the N_ν mass points and $\{w_1\}$ are the corresponding N_ν weights.

The performance of the maximum-likelihood Viterbi receiver that is mismatched in the sense that it assumes a metric that is only optimum for the linear intersymbol interference channel with additive white Gaussian noise, can be evaluated once $D_\lambda((\hat{s}_n,\hat{u}_n),(s_n,u_n))$ is known for all pairs of states $(\hat{s}_n,s_n)$ and pairs of data symbols $(\hat{u}_n,u_n)$. The effects of the nonlinear satellite channel appear in the satellite output samples z_{nc} and z_{ns}. In addition, to intersymbol interference, this same formulation can be applied to all modulations where the signal during any T-second time interval is characterized by a state and a data symbol. Here the sample correlation receiver previously discussed may also be mismatched for the linear channel but the overall analysis described in Appendix A of Part IV would still apply.

We now return to our example of BPSK modulation (M=2) and a 3-pole Butterworth transmit filter whose equivalent low-pass version has the impulse response given in (III.4.48). The receiver is the mismatched maximum-likelihood receiver for the linear channel that is realized by a Viterbi algorithm. Although this analysis applies to any AM/AM and AM/PM functions for the satellite channel model, we shall again assume the hard-limiter satellite channel model [see (III.2.14)]. In this case x_{nc} and x_{ns} as given by (III.4.45) become

$$x_c(s_n,u_n) = A\tilde{u}_n\tilde{p}(t^*) + A\sum_{i=1}^{\nu}\tilde{u}_{n-i}\tilde{p}_i(t^*)$$

$$x_s(s_n,u_n) = 0 \tag{III.4.96}$$

where $\dot{u}_n$ is again the ±1 equivalent of u_n as defined in (III.4.53), and the state s_n is characterized by the previous ν u_n's. Thus, in this case $D_\lambda((\hat{s}_n,\hat{u}_n),(s_n,u_n))$ simplifies to

$$D_\lambda\left((\hat{s}_n,\hat{u}_n),(s_n,u_n)\right) = \exp\left\{\frac{\lambda^2 N_0 d}{2T}\left[x_c(s_n,u_n) - x_c(s_n,u_n)\right]^2\right\}$$

$$\cdot\sum_{i=1}^{N_\nu}\sum_{j=1}^{N_\nu} w_1 w_j \exp\left\{\lambda\left[z_c(s_n,u_n;N_1,N_j)\left(x_c(s_n,u_n) - x_c(s_n,u_n)\right)\right]\right\}$$

$$\tag{III.4.97}$$

ORIG
OF POOR QUALITY

where

$$z_{nc} = z_c(s_n, u_n; N_i, N_j)$$

$$= \gamma \frac{x_c(s_n, u_n) + N_i}{\sqrt{\left(x_c(s_n, u_n) + N_i\right)^2 + \left(x_s(s_n, u_n) + N_j\right)^2}}$$

$$= \gamma \frac{A\tilde{u}_n \tilde{p}(t*) + A \sum_{i=1}^{\nu} \tilde{u}_{n-i} \tilde{p}_i(t*) + N_i}{\sqrt{N_j^2 + \left[A\tilde{u}_n \tilde{p}(t*) + A \sum_{i=1}^{\nu} \tilde{u}_{n-i} \tilde{p}_i(t*) + N_i\right]^2}}$$

(III.4.98)

Alternately, in terms of the normalized Chernoff parameter $\lambda_0 = \lambda \sqrt{A^2 N_{0d}/2T}$ and the uplink and downlink signal-to-noise ratio of (III.4.55) and (III.4.59), we have*

$$D_{\lambda_0}\left((\hat{s}_n, \hat{u}_n), (s_n, u_n)\right) = \frac{1}{\pi} \exp\left\{\lambda_0^2 \left[(\hat{u}_n - u_n)\tilde{p}(t*) + \sum_{i=1}^{\nu} (\hat{u}_{n-i} - u_{n-i})\tilde{p}_i(t*)\right]^2\right\}$$

$$\times \sum_{i=1}^{N_\nu} \sum_{j=1}^{N_\nu} w_i' w_j' \exp\left\{2\lambda_0\sqrt{\rho_d} \frac{\sqrt{\frac{\rho_u}{2\alpha}}\left[u_n \tilde{p}(t*) + \sum_{i=1}^{\nu} u_{n-i} \tilde{p}_i(t*)\right] + N_i'}{\sqrt{N_j'^2 + \left|\sqrt{\frac{\rho_u}{2\alpha}}\left[u_n \tilde{p}(t*) + \sum_{i=1}^{\nu} u_{n-i} \tilde{p}_i(t*)\right] + N_i'\right|^2}}\right.$$

$$\times \left.\left[(\hat{u}_n - u_n)p(t*) + \sum_{i=1}^{\nu} (\hat{u}_{n-i} - u_{n-i})\tilde{p}_i(t*)\right]\right\}$$

(III.4.99)

where the primes on N_i, N_j and w_i, w_j refer to the normalizations of (III.4.22), i.e., those values tabulated in Appendix B of [43].

---
*For simplicity of notation, we herein omit the "$\wedge$" superscripts on the u_i's with the understanding that we are talking about $\cdot$l random variables.

72

For purposes of numerical evaluation, we shall assume a value of BT that results in $\nu = 1$, i.e., only a single intersymbol interference sample. Then, defining the paired state $\mathscr{S}_n \overset{\Delta}{=} (u_n, \hat{u}_n)$ and using the transfer function bound approach as described in Appendix A of Part IV, we arrive at the transfer function state diagram of Figure 16a or its reduced version as in Figure 16b whereupon

$$T(z; \lambda_0) = \frac{(a+b)(f+h)}{[1 - (c+d)]} \qquad (III.4.100)$$

with

$$a = \frac{z}{2} D_{\lambda_0}\Big((+1,+1),(+1,-1)\Big) = \frac{z}{2} D_{\lambda_0}\Big((-1,-1),(-1,+1)\Big) \overset{\Delta}{=} a_0 z$$

$$b = \frac{z}{2} D_{\lambda_0}\Big((+1,+1),(-1,+1)\Big) = \frac{z}{2} D_{\lambda_0}\Big((-1,-1),(+1,-1)\Big) \overset{\Delta}{=} b_0 z$$

$$c = \frac{z}{2} D_{\lambda_0}\Big((+1,-1),(+1,-1)\Big) = \frac{z}{2} D_{\lambda_0}\Big((-1,+1),(-1,+1)\Big) \overset{\Delta}{=} c_0 z$$

$$d = \frac{z}{2} D_{\lambda_0}\Big((+1,-1),(-1,+1)\Big) = \frac{z}{2} D_{\lambda_0}\Big((-1,+1),(+1,-1)\Big) \overset{\Delta}{=} d_0 z$$

$$f = \frac{1}{2} D_{\lambda_0}\Big((+1,-1),(+1,+1)\Big) = \frac{1}{2} D_{\lambda_0}\Big((-1,+1),(-1,-1)\Big)$$

$$h = \frac{1}{2} D_{\lambda_0}\Big((+1,-1),(-1,-1)\Big) = \frac{1}{2} D_{\lambda_0}\Big((-1,+1),(+1,+1)\Big)$$

$$(III.4.101)$$

In (III.4.101),

$$D_{\lambda_0}\Big((u_{k-1}, u_{k-1}),(u_k, \hat{u}_k)\Big) = D_{\lambda_0}(\mathscr{S}_{k-1}, \mathscr{S}_k) \qquad (III.4.102)$$

is obtained by evaluating (III.4.99) with the appropriate values of $u_{n-1}, u_n, \hat{u}_{n-1}$, and u_n. Finally, the bit error bound is given by
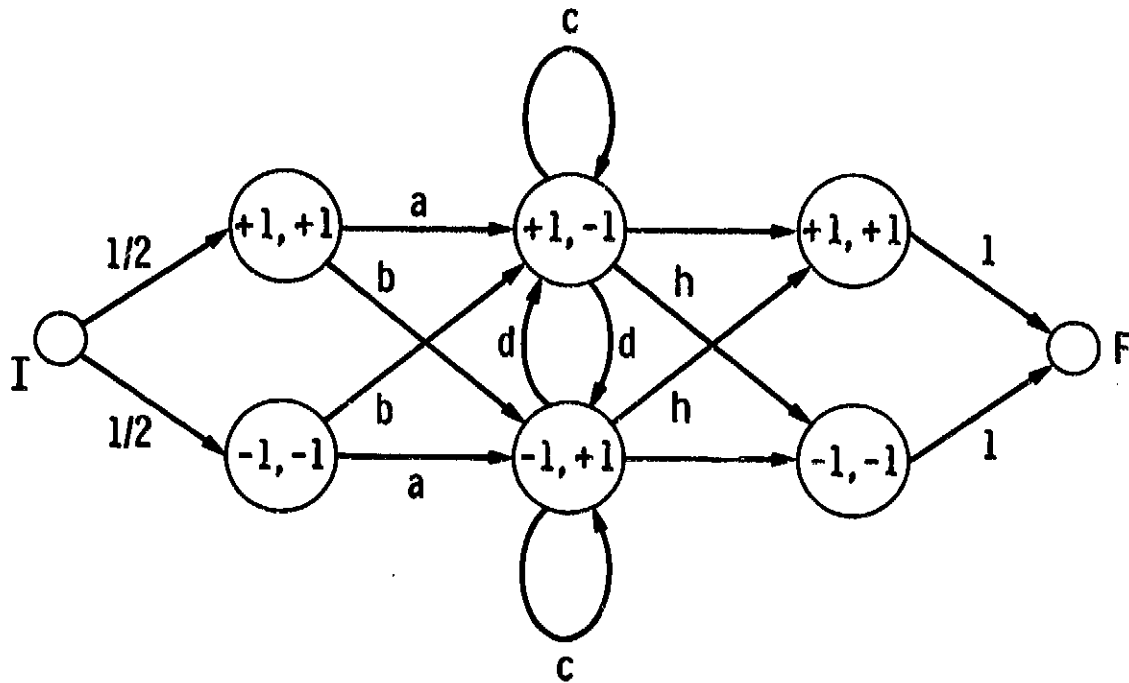
Figure 16a.   Transfer Function State Diagram
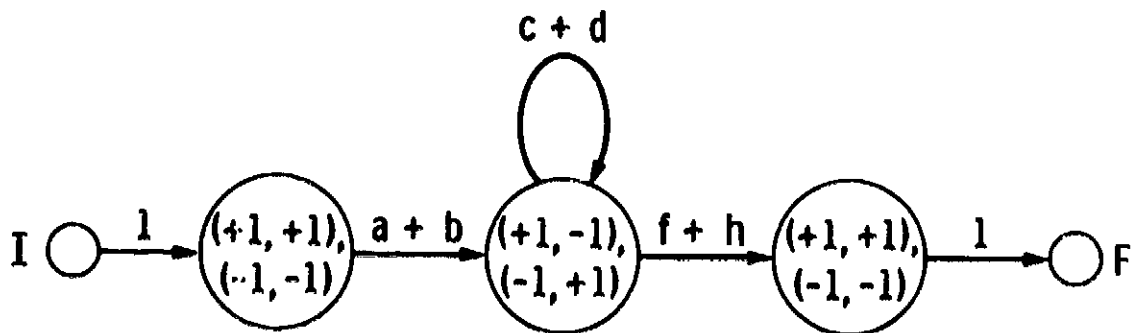
Figure 16b.   Reduced Transfer Function State Diagram

74

$$P_b \doteq \min_{\lambda_0} \frac{1}{2} \left. \frac{dT(z;\lambda_0)}{dz} \right|_{z=1} \tag{III.4.103}$$

where from (III.4.100)

$$\left. \frac{dT(z;\lambda_0)}{dz} \right|_{z=1} = \frac{(a_0+b_0)\,(f+h)}{\left[1-(c_0+d_0)\right]^2} \tag{III.4.104}$$

Figure 17 is a plot of the upper bound of (III.4.104) versus downlink signal-to-noise ratio ρ_d with uplink signal-to-noise ratio ρ_u as a parameter. The value BT=1 was chosen so as to satisfy the requirement of a single interfering sample. Comparing these results with those of Figure 11 for the memoryless receiver, we observe that the upper bound as computed from (III.4.104) is extremely loose. This is an unfortunate consequence of the Chernoff bound approach when the uplink signal-to-noise ratio is not very large. The transfer function bound can be tightened somewhat using an approach in [34; Appendix C]. Unfortunately, even this modification is not sufficiently tight when uplink noise is present and intersymbol interference is small. The conclusion to be reached is that the transfer function bound approach is useful for calculating the performance of mismatched receivers of the MLSE type only in the "absence" of uplink noise when the intersymbol interference is small, or in the presence of uplink noise and intersymbol interference when the latter is the dominant degrading effect.

When the transmitted signal is a staggered quadrature modulation of the form in (III.4.78), then one can envision two possible structures for the mismatched Viterbi receiver. In one case, separate and identical Viterbi demodulators are used to process the output samples of each of the two quadrature channels. In the more general case, a single mismatched receiver (analogous to Figure 9) forms its metric from the combination of the two staggered sample sets, thus treating each data pair (a_n, b_n) as the symbol u_n to be detected. Assuming, as for the BPSK example, a 3-pole Butterworth transmit filter and hard limited

75
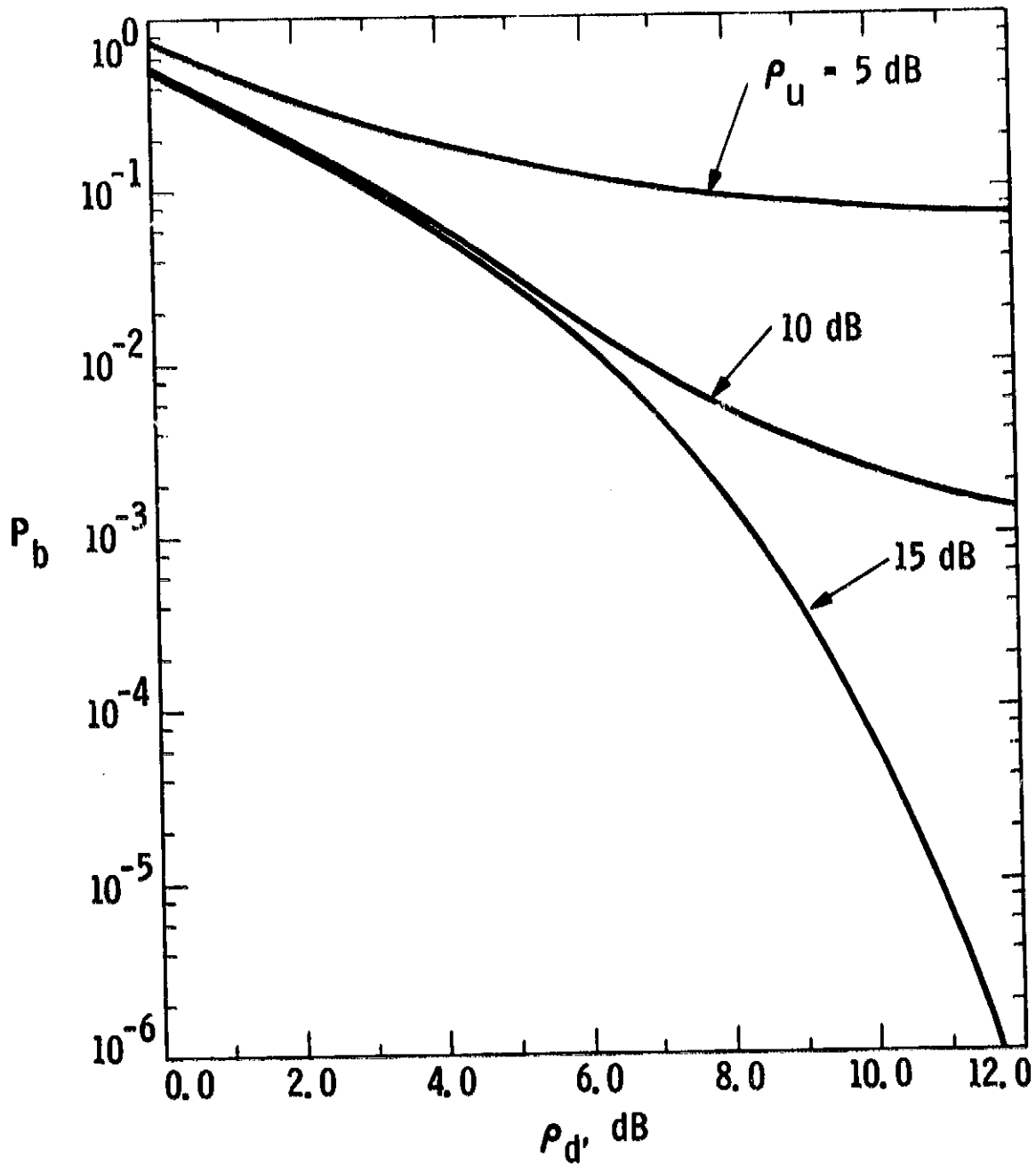
Figure 17.   Upper Bounds on the Bit Error Probability Performance of
the Maximum-Likelihood Sequence Estimation Receiver for
BPSK Transmitted over a Hard-Limited Intersymbol Inter-
ference Channel; BT = 1.

satellite channel, then for the first case, we have analogous to (III.4.99)*

$$D_{\lambda_0}\left((s_n, a_n), (s_n, a_n)\right) = \frac{1}{a}\exp\left[\lambda_0^2(\Lambda_n - \Lambda_n)^2\right]$$

$$\cdot \sum_{i=1}^{N_v}\sum_{j=1}^{N_v} w_i' w_j' \exp\left\{2\lambda_0 \sqrt{\rho_d} \frac{\left(\sqrt{\frac{\rho_u}{2\alpha}}\Lambda_n + N_1'\right)\left(\Lambda_n - \Lambda_n\right)}{\sqrt{\left(\sqrt{\frac{\rho_u}{2\alpha}}B_n + N_1'\right)^2 + \left(\sqrt{\frac{\rho_u}{2\alpha}}\Lambda_n + N_1'\right)^2}}\right\}$$

(III.4.105)

where

$$\Lambda_n \triangleq \frac{x_c(s_n, a_n)}{\Lambda} = a_n p(t\star) + \sum_{i=1}^{\nu} a_{n-i} p_{2i}(t\star)$$

$$B_n = \sum_{i=1}^{\nu} b_{n-i} p_{2i-1}(t\star)$$

(III.4.106)

Here the state s_n corresponds to $\{a_{n-i}; i=1,2,\ldots\nu\}$ and does not include the $\{b_n\}$ sequence. Suppose that the value of BT is chosen such that only one intersymbol interference and two cross-interference terms are significant. Then, the first term of the square root in (III.4.105) can be written in the form

$$\left(\sqrt{\frac{\rho_u}{2\alpha}}B_n + N_1'\right)^2 = \left(\sqrt{\frac{\rho_u}{2\alpha}}[b_{n-1}p_1(t\star) + b_{n-2}p_3(t\star)] + N_1'\right)^2$$

$$= \left(\sqrt{\frac{\rho_u}{2\alpha}}[p_1(t\star) + b_{n-2}b_{n-1}p_3(t\star)] + b_{n-1}N_1'\right)^2$$

(III.4.107)

*We assume here that a_n corresponds to a_n with the data $\{b_n\}$ producing only cross-channel interference. Because of the symmetry of the problem, an identical result is obtained for the quadrature channel if the a_n's are replaced by b_n's and vice versa.

or since b_{n-2} b_{n-1}, is just another i.i.d. sequence (say $\{c_n\}$) and Gauss-quadrature averaging over b_{n-1} N_j' is identical to Gauss-quadrature averaging over N_j', we get

$$\left(\sqrt{\frac{\rho_u}{2\alpha}}\, B_n + N_j'\right)^2 - \left(\sqrt{\frac{\rho_u}{2\alpha}}\, [p_1(t*) + c_n p_3(t*)] + N_j'\right)^2$$

(III.4.198)

Thus, to compute the bit error probability performance of the staggered quadrature system, the transfer function bound of (III.4.103) together with (III.4.104) is still appropriate. Here, however, we evaluate each term in (III.4.191) using (III.4.105) averaged over the two possible values (± 1) of c_n. Figure 18 illustrates the results for an SQORC modulation with $BT = 1$. Again comparison of these results with those for the memoryless receiver (see Figure 14) unfortunately reveals the looseness of the bound.

To conclude this section, we point out that the notion of mismatched receiver can be generalized to include cases where the receiver has memory but less than that of the channel. For example, suppose that we consider the same intersymbol interference BPSK modulation examined above but now the Viterbi algorithm's complexity is reduced by assuming intersymbol interference memory $\hat{\nu} < \nu$ where ν is the actual memory in data symbols due to the 3-pole Butterworth filter. An analysis of this case is given in [35] with numerical results illustrated for a range of BT values and mismatches $\hat{\nu} \neq \nu$.

4.1.1.3   Approximate Optimum Maximum-Likelihood Receivers

In the previous section, we assumed a mismatched maximum-likelihood receiver that did not account for the nonlinearity of the satellite channel. We now consider the ideal maximum-likelihood receiver which is matched to the channel and then consider an approximate form of it using the Gauss-Hermite quadrature formula.

Assuming the same notation as in the previous section, the conditional probability of y_n given state s_n, data symbol $\hat{u}_n$, and the uplink noise components n_{nc} and $\hat{n}_{ns}$, has the form

78
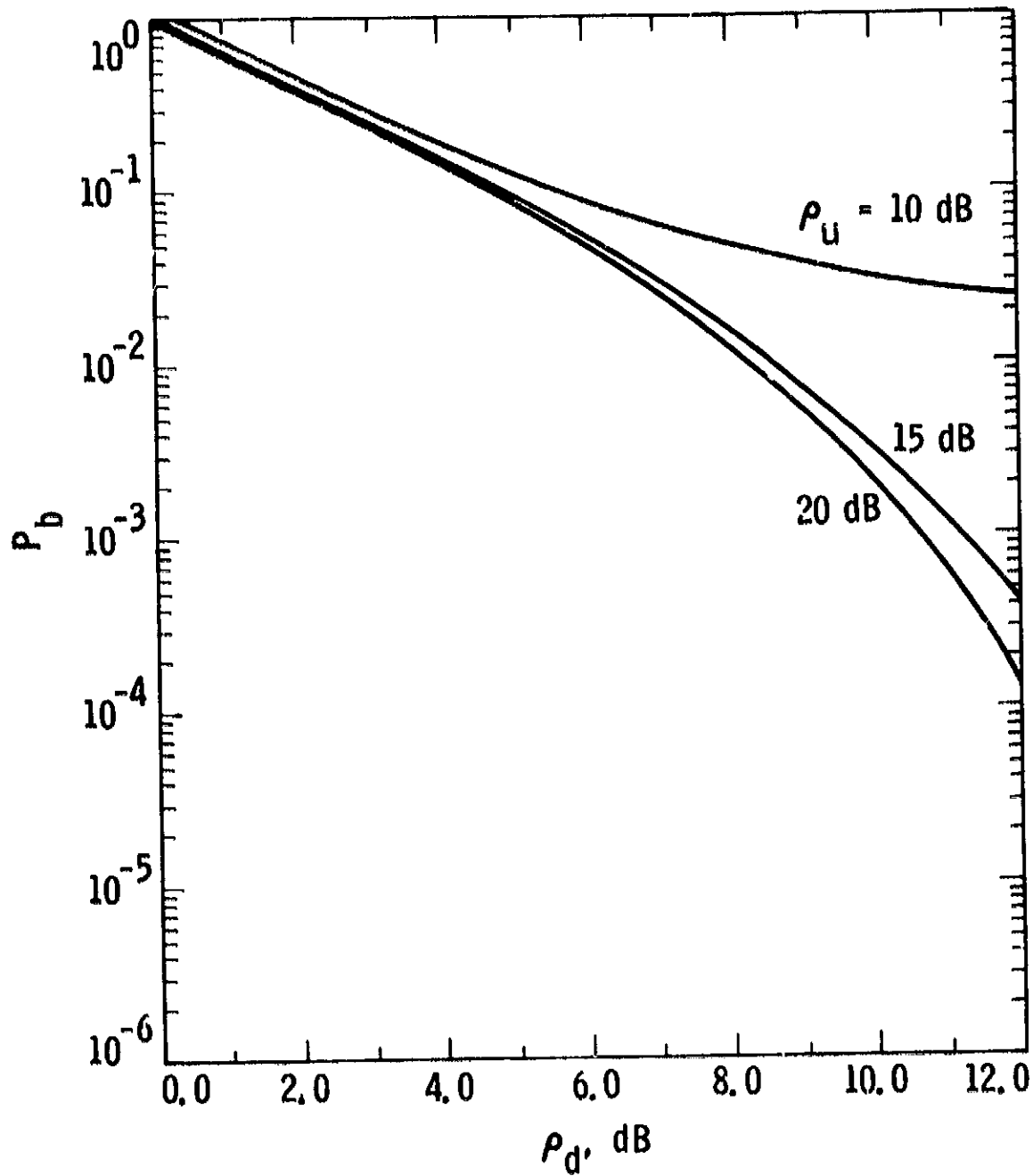
Figure 18. Upper Bounds on the Bit Error Probability Performance of the Maximum-Likelihood Sequence Estimation Receiver for SQORC Modulation Transmitted over a Hard-Limited Intersymbol Interference Channel; $BT = 1$.

$$p(y_n | \hat{s}_n, \hat{u}_n; \tilde{n}_{nc}, \tilde{n}_{ns}) = \frac{1}{2\pi N_{0d}/T}$$

$$\times \exp \left\{ -\frac{[y_{nc} - z_c(\hat{s}_n, \hat{u}_n; \tilde{n}_{nc}, \tilde{n}_{ns})]^2 + [y_{ns} - z_s(\hat{s}_n, \hat{u}_n; \tilde{n}_{nc}, \tilde{n}_{ns})]^2}{2N_{0d}/T} \right\}$$

(III.4.109)

This follows immediately from the fact that if $\hat{s}_n$, $\hat{u}_n$, $\tilde{n}_{nc}$, and $\tilde{n}_{ns}$ are all given, then $z_{nc} = z_c(\hat{s}_n, \hat{u}_n; \tilde{n}_{nc}, \tilde{n}_{ns})$ and $z_{ns} = z_s(\hat{s}_n, \hat{u}_n; \tilde{n}_{nc}, \tilde{n}_{ns})$ are known and

$$p(y_n | z_n) = \frac{1}{2\pi N_{0d}/T} \exp \left\{ -\frac{\| y_n - z_n \|^2}{2N_{0d}/T} \right\}$$

(III.4.110)

Next if we assume that only $\hat{s}_n$ and $\hat{u}_n$ are given, then the conditional probability of y_n is obtained by averaging (III.4.109) over the independent uplink Gaussian noise components $\tilde{n}_{nc}$ and $\tilde{n}_{ns}$, i.e.,

$$p(y_n | \hat{s}_n, \hat{u}_n) = E \left\{ p(y_n | \hat{s}_n, \hat{u}_n; \tilde{n}_{nc}, \tilde{n}_{ns}) \right\}$$

(III.4.111)

For a sequence of data symbols $\hat{u}$, the conditional probability of $y_1, y_2, \ldots, y_N$ is given by

$$p(y_1, y_2, \ldots, y_N | \hat{u}) = \prod_{k=1}^{N} p(y_k | \hat{s}_k, \hat{u}_k)$$

(III.4.112)

and thus by taking the natural logarithm we obtain

$$\ln p(y_1, y_2, \ldots, y_N | \hat{u}) = \sum_{k=1}^{N} m(y_k; \hat{s}_k, \hat{u}_k)$$

(III.4.113)

where

$$m(y_k;s_k,u_k) \triangleq \ln p(y_k|s_k,u_k) \qquad (III.4.114)$$

is the optimum maximum-likelihood metric.

We next approximate the maximum-likelihood metric by approximating the expectation in (III.4.111) with the Gauss-Hermite quadrature formula

$$\hat{p}(y_n|\hat{s}_n,\hat{u}_n) \triangleq \sum_{i=1}^{L}\sum_{j=1}^{L} w_i w_j \ p(y_n|\hat{s}_n,\hat{u}_n;N_i,N_j) \qquad (III.4.115)$$

The accuracy of this approximation depends on the parameter L. (The choice of L=1 coincides with the optimum maximum-likelihood metric assuming no uplink noise). The approximate maximum-likelihood metric is thus

$$\hat{m}(y_n;\hat{s}_n,\hat{u}_n) = \ln \hat{p}(y_n|\hat{s}_n,\hat{u}_n). \qquad (III.4.116)$$

For this metric, the parameter D_λ is given by (III.3.9) where the expectation is over the uplink and downlink noise components in the vector

$$y_n = \begin{bmatrix} z_c(s_n,u_n;n_{nc},n_{ns}) + n_{nc} \\ z_s(s_n,u_n;n_{nc},n_{ns}) + n_{ns} \end{bmatrix} \qquad (III.4.117)$$

To emphasize this dependence we write

$$y_n = y(s_n,u_n;n_{nc},n_{ns};n_{nc},n_{ns}) \qquad (III.4.118)$$

Then

$$D_\lambda((s_n,u_n),(s_n,u_n)) = E\left\{ \exp\left[\lambda\left(m(y(s_n,u_n;n_{nc},n_{ns},n_{nc},n_{ns});s_n,u_n) \right.\right.\right.$$
$$\left.\left.\left. - m(y(s_n,u_n;n_{nc},n_{ns};n_{nc},n_{ns});s_n,u_n) \right) \right] \right\} \qquad (III.4.119)$$

81

Again we can use the Gauss-Hermite quadrature formula for the independent Gaussian random variables $\hat{n}_{nc}$, $\hat{n}_{ns}$, n_{nc}, and n_{ns} which results in*

$$D_\lambda((\hat{s}_n,\hat{u}_n),(s_n,u_n)) = \sum_{i=1}^{N_\nu}\sum_{j=1}^{N_\nu}\sum_{k=1}^{N_\nu}\sum_{\ell=1}^{N_\nu} w_i w_j w_k w_\ell$$

$$\times \exp\left[\lambda\left(\hat{m}(\underline{y}(s_n,u_n;N_i,N_j;N_k,N_\ell);\hat{s}_n,\hat{u}_n)\right.\right.$$

$$\left.\left. -\hat{m}(\underline{y}(s_n,u_n;N_i,N_j;N_k,N_\ell);s_n,u_n)\right)\right]$$

$$(III.4.120)$$

Numerical illustrations of the application of (III.4.120) to computing average bit error probability performance using the transfer function bound approach are discussed in detail in [40]. For example, a digital satellite link using BPSK signaling and an on-board TWT amplifier with AM/AM and AM/PM characteristics illustrated in Figure 19 was considered. The linear part of the channel was assumed to have an impulse response with intersymbol interference of memory one and a ratio of interfering sample to pulse peak equal to 0.5. The TWT is assumed to operate at saturation in the absence of noise and intersymbol interference. Figure 20 illustrates the behavior of the ML receiver by plotting the pairs of uplink and downlink signal-to-noise ratio values that allow a bit error probability of 10^{-4}. The two continuous curves represent the approximate ML receiver as discussed above with $L=3$ and $L=7$. For the sake of comparison, the performance for the linear case, in which the uplink and downlink noises simply sum up without the enhancement effect due to the nonlinear device, is illustrated in same figure by the dashed line curve. Also shown is a dotted line

---

*Note that the number L of approximating terms used in arriving at the approximate metric of (III.4.116) is not constrained to be equal to the number N_ν of the approximating terms used in performing the four averages in (III.4.120). Typically, a value of L less than N_ν is adequate.
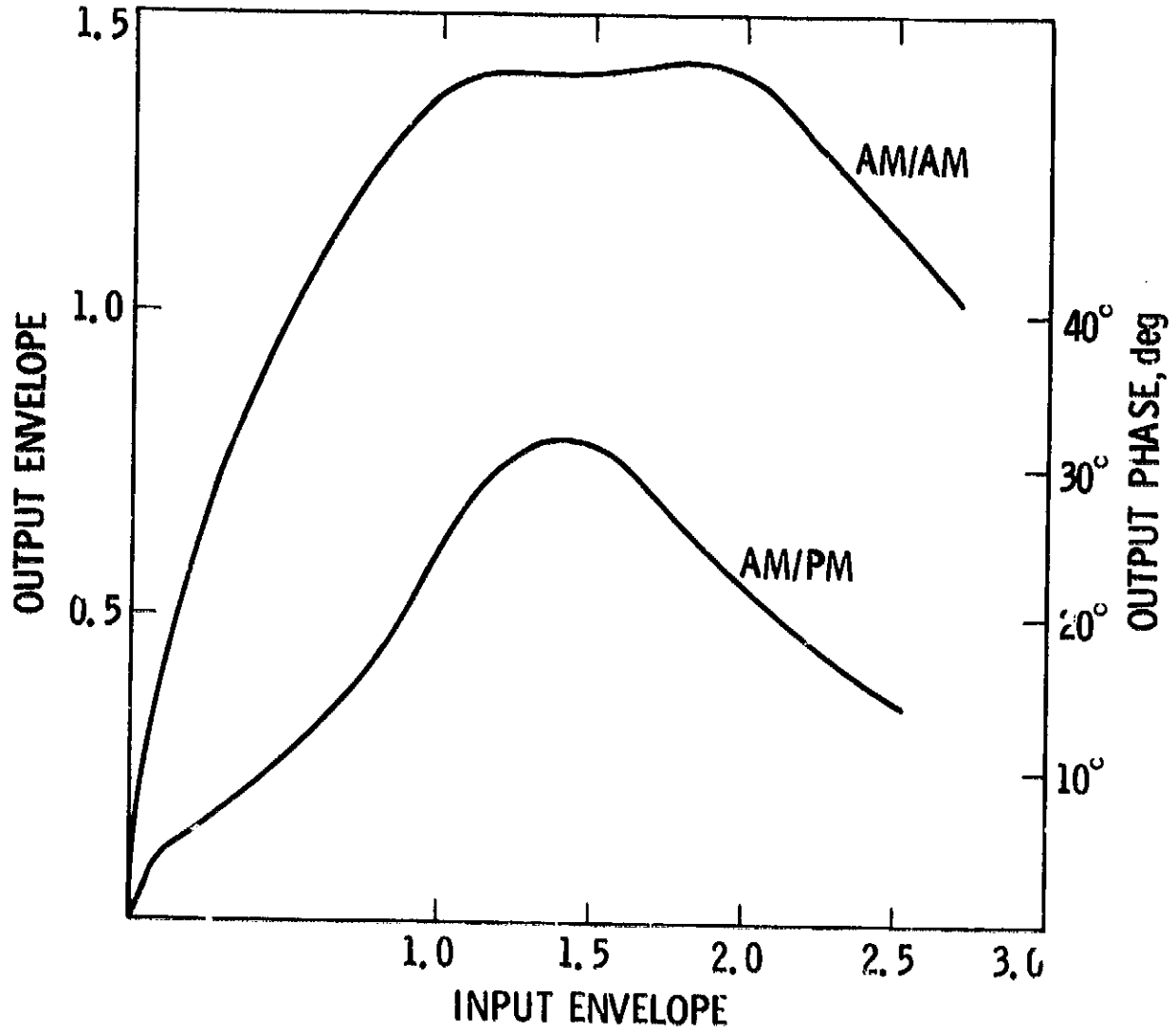
Figure 19. AM/AM and AM/PM Characteristics
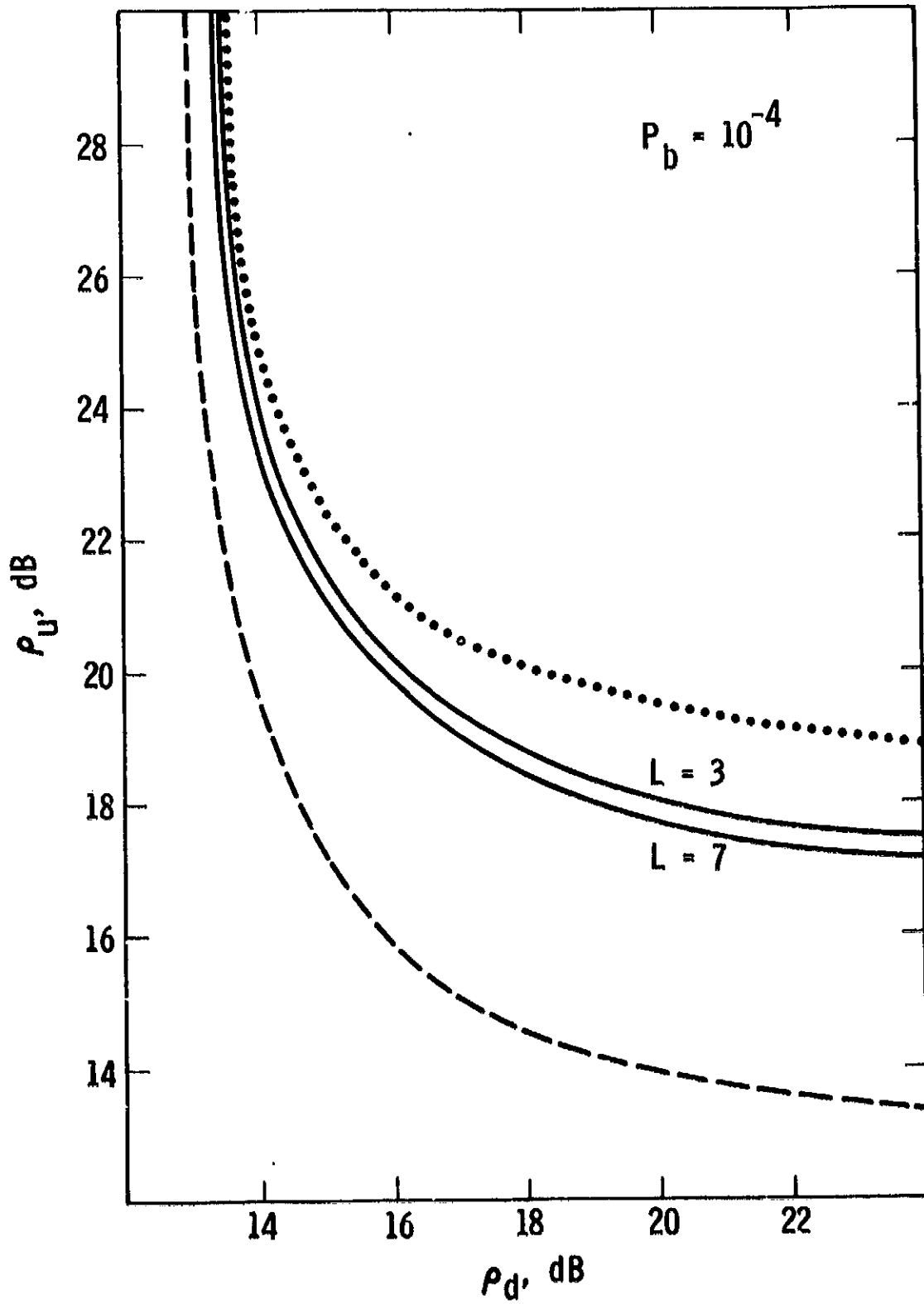
Figure 20. Required Uplink and Downlink Signal-to-Noise Ratios for $P_b = 10^{-4}$; Approximate Maximum-Likelihood Receiver

curve which corresponds to the receiver using a ML strategy but designed without taking into account the presence of uplink noise.

The two continuous curves show that the rough approximation with L=3, which leads to a very simple receiver, is close to optimum since it is very close to the L=7 curve. Moreover, it is seen that even the simple approximate ML receiver allows a saving of more than 1 dB, in some situations, with respect to the conventional one.

REFERENCES

[1]   Shimbo, O., Fang, R., and Celebiler, M., "Performance of M-ary PSK systems
      in Gaussian noise and intersymbol interference," IEEE Transactions on In-
      formation Theory, vol. IT-19, January 1973, pp. 44-58.

[2]   Fang, R., and Shimbo, O., "Unified analysis of a class of digital systems
      in additive noise and interference," IEEE Transactions on Communications,
      vol. COM-21, October 1973, pp. 1075-1091.

[3]   Ekanayake, N., and Taylor, D.P., "CPSK signaling over hard-limited channels
      in additive gaussian noise and intersymbol interference," IEEE Transactions
      on Information Theory, vol. IT-25, no. 1, January 1979, pp. 62-68.

[4]   Jain, P.C., and Blachman, N.M., "Detection of a PSK signal transmitted
      through a hard-limited channel," IEEE Transactions on Information Theory,
      vol. IT-19, September 1973, pp. 623-630.

[5]   Sunde, E.D., "Intermodulation distortion in multicarrier FM systems," in
      IEEE International Convention Record, 1965, vol. 13, pt. 2, pp. 130-146.

[6]   Berman, A.L., and Mahle, C.H., "Nonlinear phase shift in traveling wave
      tubes as applied to multiple access communication satellites," IEEE Transac-
      tions on Communication Technology, vol. COM-18, February 1970, pp. 37-48.

[7]   Shimbo, O., "Effects of intermodulation, AM-PM conversion, and additive
      noise in multicarrier TWT systems," Proceedings of the IEEE, vol. 59,
      February 1971, pp. 230-238.

[8]   Thomas, C.M., Weidner, M.Y., and Durrani, S.H., "Digital amplitude-phase
      keying with M-ary alphabets," IEEE Transactions on Communications, vol.
      COM-22, February 1974, pp. 168-180.

[9]   Kaye, A.R., George, D.A., and Eric, M.J., "Analysis and compensation of
      bandpass nonlinearities for communications," IEEE Transactions on Communi-
      cation Technology, vol. COM-20, October 1972, pp. 965-972.

[10] Eric, M.J., "Intermodulation analysis of nonlinear devices for multiple
      carrier inputs," Communications Research Centre, Ottawa, Ontario, Canada,
      CRC Rep. 1234, November 1972.

[11] Hetrakul, P., and Taylor, D.P., "Nonlinear quadrature model for a traveling-
      wave-tube-type amplifier," Electronics Letters, vol. 11, January 23, 1974,
      p. 50.

[12] _____, "The effects of transponder nonlinearity on binary CPSK signal trans-
      mission," IEEE Transactions on Communications, vol. COM-24, May 1976, pp.
      546-553.

[13] _____, "Compensators for bandpass nonlinearities in satellite communica-
      tions," IEEE Transactions on Aerospace and Electronic Systems, vol. AES-12,
      July 1976, pp. 509-514.

[14] Saleh, A.A.M., "Frequency-independent and frequency-dependent nonlinear models of TWT amplifiers," IEEE Transactions on Communications, vol. COM-29, no. 11, November 1981, pp. 1715-1720.

[15] Fuenzalida, J.C., Shimbo, O., and Cook, W.L., "Time-domain analysis of intermodulation effects caused by nonlinear amplifiers," COMSAT Technical Review, vol. 3, Spring 1973, pp. 89-143.

[16] Lyon, R.G., "The effect of a bandpass nonlinearity on signal detectability," IEEE Transactions on Communications, vol. COM-21, no. 1, January 1973, pp. 51-60.

[17] Lindsey, W.C., Omura, J.K., Woo, K.T., Huang, T.C., and Biederman, L., "Investigation of modulation/coding trade-off for military satellite communications," volumes I, II, and III, LinCom Corporation, P.O. Box 2793D, Pasadena, CA, July 19, 1977.

[18] Jain, P., Huang, T.C., Woo, K.T., and Omura, J.K., "Detection of MPSK signals transmitted through a nonlinear satellite repeater," NTC '77 Conference Record, Los Angeles, California, December 5-7, 1977, pp. 26:2-1 - 26:2-4.

[19] Biederman, L., and Omura, J.K., "Performance of Viterbi demodulators for nonlinear satellite channels with intersymbol interference," NTC '77 Conference Record, Los Angeles, California, December 5-7, 1977, pp. 26:6-1 - 26:6-6.

[20] _____, "The computational cut-off rate for nonlinear ISI channels," NTC '77 Conference Record, Los Angeles, California, December 5-7, 1977, pp. 36:5-1 - 36:5-6.

[21] Huang, T.C., Omura, J.K., and Lindsey, W.C., "Analysis of coherent satellite communication systems in the presence of interference and noise," IEEE Transactions on Communications, vol. COM-29, No. 5, May 1981, pp. 593-604.

[22] Viterbi, A.J., "Error bounds for convolutional codes and an asymptotically optimum decoding algorithm," IEEE Transactions on Information Theory, vol. IT-13, April 1967, pp. 260-269.

[23] Forney, G.D., Jr., "Maximum-likelihood sequence estimation of digital sequences in the presence of intersymbol interference," IEEE Transactions on Information Theory, vol. IT-18, May 1972, pp. 363-378.

[24] Ungerboeck, G., "Adaptive maximum-likelihood receiver for carrier-modulated data transmission systems," IEEE Transactions on Communications, vol. COM-22, May 1974, pp. 624-636.

[25] Hayes, J.F., "The Viterbi algorithm applied to digital data transmission," Communication Society Magazine, vol. 13, March 1975, pp. 15-20.

[26] Mesiya, M.F., McLane, P.J., and Campbell, L.L., "Maximum-likelihood sequence estimation of binary sequences transmitted over band-limited nonlinear channels," IEEE Transactions on Communications, vol. COM-25, July 1977, pp. 633-643.

[27] Forsey, R.J., Gooding, V.E., McLane, P.J., and Campbell, L.L., "M-ary PSK transmission via a coherent two-link channel exhibiting AM-AM and AM-PM nonlinearities," in Proceedings of International Conference on Communications, ICC '77, Chicago, IL, June 12-15, 1977, pp. 16.2-335 to 16.2-339.

[28] Falconer, D.D., and Magee, F.R., Jr., "Adaptive channel memory truncation for maximum-likelihood sequence estimation," Bell System Technical Journal, vol. 52, November 1973, pp. 1541-1562.

[29] Qureshi, S., and Newhall, E., "An adaptive receiver for data transmission over time-dispersive channels," IEEE Transactions on Information Theory, vol. IT-19, July 1973, pp. 448-457.

[30] Lee, W.U., and Hill, F.S., Jr., "A maximum-likelihood sequence estimator with decision feedback equalization," IEEE Transactions on Communications, vol. COM-25, September 1977, 971-980.

[31] Vermeulen, F.L., and Hellman, M.E., "Reduced state Viterbi detectors for channels with intersymbol interference," ICC'74 Conference Record, San Francisco, CA, June 1974, pp. 37B-1 - 37B-4.

[32] Foschini, G.J., "A reduced state variant of maximum-likelihood sequence detection attaining optimum performance at high signal-to-noise ratios," IEEE Transactions on Information Theory, vol. IT-23, September 1977, pp. 605-609.

[33] Divsalar, D., and Omura, J.K., "Performance of intersymbol interference channels under mismatch conditions," ICC'78 Conference Record, Toronto, Canada, June 4-7, 1978, pp. 30.3.1 - 30.3.5.

[34] Divsalar, D., "Performance of mismatched receivers on bandlimited channels," Ph.D. Thesis, University of California at Los Angeles, 1978.

[35] Divsalar, D., "Performance of mismatched Viterbi receiver on satellite channels," ICC'79 Conference Record, Boston, MA, June 10-14, 1979, pp. 34.3.1 - 34.3.5.

[36] McLane, P., "A residual intersymbol interference error bound for truncated-state Viterbi detectors," IEEE Transactions on Information Theory, vol. IT-26, no. 5, September 1980, pp. 548-553.

[37] Lawless, W.J., and Schwartz, M., "Binary signalling over channels containing quadratic nonlinearities," IEEE Transactions on Communications, vol. COM-22, March 1974, pp. 288-299.

[38] Taylor, D.P., and Hetrakul, P., "Receiver structure for saturating channels," IEEE Transactions on Communications, vol. COM-26, February 1978, pp. 270-277.

[39] Benedetto, S., Biglieri, E., and Omura, J.K., "Maximum-likelihood sequence estimation for nonlinear satellite channels with uplink and downlink noise," ICC'80 Conference Record, Seattle, Washington, June 8-12, 1980, pp. 62.2.1-62.2.5.

[40] Benedetto, S., Biglieri, E., and Omura, J.K., "Optimum receivers for non-linear satellite channels," 5th International Conference on Digital Satellite Communications, Genoa, Italy, March 23-26, 1981.

[41] Lesh, J.R., Guest Editor of "Special section on communications over non-linear channels," IEEE Transactions on Communications, vol. COM-29, no. 5, May 1981, pp. 537-620.

[42] Omura, J.K., and Simon, M.K., "Satellite communication performance evaluation: computational techniques based on moments," JPL Publication 80-7L, Jet Propulsion Laboratory, Pasadena, CA, September 15, 1980.

[43] Krylov, V.I., Approximate Calculation of Integrals, translated by A.H. Shroud, MacMillen, New York, 1962.

[44] Massey, J.L., "Shift register synthesis and BCH decoding," IEEE Transactions on Information Theory, vol. IT-15, no. 1, January 1969, pp. 122-127.

[45] Austin, M.C., and Chang, M.U., "Quadrature overlapped raised-cosine modulation," IEEE Transactions on Communications, vol. COM-29, no. 3, March 1981, pp. 237-249.

[46] Divsalar, D., and Simon, M.K., "Performance of quadrature overlapped raised-cosine modulation over nonlinear satellite channels," ICC'81 Conference Record, Denver, Colorado, June 14-18, 1981, pp. 2.3.1-2.3.7.

[47] Simon, M.K., Omura, J.K., and Divsalar, D., "Performance of staggered quadrature modulations over nonlinear satellite channels with uplink noise and intersymbol interference," to be presented at GLOBECOM'82, November 29-December 2, 1982, Miami, Florida.

[48] Doelz, M.L., and Heald, E.H., "Minimum-shift data communication systems," U.S. Patent 2,977,417, March 28, 1961.

[49] Pasupathy, S., "Minimum-shift-keying: a spectrally efficient modulation," IEEE Communications Society Magazine, vol. 17, July 1979, pp. 14-22.